



# Authigenic potassic silicates in the Rathdowney Trend, southwest Ireland: New perspectives for ore genesis from petrography of gangue phases in Irish-type carbonate-hosted Zn-Pb deposits



T. Riegler\*, S.H. McClenaghan

Department of Geology, Museum Building, Trinity College Dublin, Dublin 2, Ireland

Irish Center for Research in Applied Geosciences, UCD School of Geological Sciences, Belfield, Dublin 4, Ireland

## ARTICLE INFO

### Article history:

Received 20 December 2016

Received in revised form 5 April 2017

Accepted 9 April 2017

Available online 23 April 2017

### Keywords:

Irish ore field

Lead-zinc

Potassic silicates

Breccias

## ABSTRACT

Petrographic studies of Zn-Pb ore zones hosted by Lower Carboniferous dolomitized Waulsortian reef limestones in the Rathdowney Trend reveal a paragenetic association between sphalerite and potassium silicates: (Ba, K)-feldspar, adularia, and albite as well as rare quartz, illite and phengite. The dominant mineral assemblage is composed of 1) sphalerite ± (K,Ba) feldspar ± pengite/illite near the putative feeder conduit for the Lisheen Main Zone, and 2) a sphalerite ± pengite/illite assemblage distal to the major normal faults (NW of Main Zone, Island Zone and Rapla occurrence). In addition, clay minerals have been identified in fault gouges located at the interface between the Waulsortian reef and argillaceous limestone of the Ballysteen Formation. This mineral assemblage has provided additional constraints on the physico-chemical conditions of ore formation (eH, pH, sulfur and metal species). Another implication of the mineral assemblage, is a revision of fluid rock interaction processes, in which mineral solution-precipitation reactions are contributing to the development of hydrothermal breccias, with dolomitic black matrix breccias interpreted as a by-product of massive sulfide precipitation. Additionally, textural studies of the breccias through fractal dimension analysis of fragment geometry extracted from large scale scanning electron microscope element maps (1 cm<sup>2</sup> areas or more), indicates the prevalence of chemical brecciation-corrosion processes in the generation of the black matrix breccias. Integration of these new observations allows for comparison of ore forming processes across the Irish Midlands from the perspective of gangue mineralogy and may provide further links with classic Mississippi-type deposits from the mid-continent region of the United States of America.

© 2017 Elsevier B.V. All rights reserved.

## 1. Introduction

The Irish Midlands is a world-class base-metal metallogenic province with more than 150 Mt of massive sulfides. Since the 1960s, Zn-Pb-(Ag-Cu) mineralization has been mined from five economic ore bodies hosted by Lower Carboniferous limestones, these are: Tynagh, Silvermines, Galmoy, Lisheen, and Navan (Tara Mines). The Lisheen Zn-Pb (Ag) deposit contained more than 22 Mt of ore with an overall grade of 11.5% Zn, 1.9% Pb and 26 g/t Ag as well as 16% Fe (pyrite) hosted in Lower Carboniferous Courcyeuan to Chadian Lisduff oolitic limestone of the Ballysteen Formation, and in the Waulsortian mudbank facies, the latter being the dominant ore bearing strata (Hitzman et al., 2002). At a regional scale, the stratabound Zn-Pb mineralization is structurally controlled by sets of normal ENE faults that were active during

\* Corresponding author.

E-mail address: [rieglert@tcd.ie](mailto:rieglert@tcd.ie) (T. Riegler).

sedimentation; mineralization occurs predominantly in the hanging wall of normal faults (Johnston et al., 1996). Mineralization comprises sphalerite, galena, pyrite and tennantite, and forms complex replacement ore textures including colloform fillings of dissolution vugs and polygenic breccias. Non-sulfide gangue minerals include dolomite, calcite, barite, and quartz as well as a range of silicate minerals. The Waulsortian mudbank facies was affected by regional-scale dolomitization, followed by hydrothermal dolomite alteration historically referred to as black matrix, and white matrix breccias, both associated with sulfide mineralization along the Rathdowney Trend (Cruise, 2000; Doyle et al., 1992; Hitzman et al., 1992; Redmond, 1997).

In the present work we propose to refine the overall paragenetic sequence, focusing on gangue minerals including quartz, (Ba, K) feldspars, and illite, using crystallochemical and textural evidence to constrain their textural relationship to sulfide minerals. In light of the abundant literature on carbonate-hosted Zn-Pb deposits, the main goal of this work is to integrate and use hydrothermal silicate

minerals to further characterise alteration processes and the geochemical signatures associated with the precipitation of massive sulfides (primary or secondary from remobilization) along the Rathdowney Trend. The study focuses on silicate occurrences from the proximal feeder zone at Lisheen (Killoran fault at the South of Main Zone) to distal or isolated pods of mineralization in the Island Ore Zone and the Rapla prospect. We also aim to add petrographic and genetic constraints on ore-related breccias including the equivocal classification of black matrix breccias (BMB), through the fractal analysis of fragments. In light of the new micro-analytical data and petrological constraints we aim to contribute to the understanding of ore forming processes responsible for the Zn-Pb mineralization in the Irish Midlands.

### 1.1. Host rock alteration in carbonate hosted Zn-Pb mineralization

Alteration mineral assemblages within host rock strata are important for placing constraints on physico-chemical conditions of ore forming fluids (e.g. pH, eH, activity and form of S, and metals). The mineralogical expression of hydrothermal alteration in carbonate-hosted Zn-Pb mineralization can be broadly divided into two main types: non-silicate and silicate. These alteration styles have been described for a wide range of world-class lead zinc districts e.g. Midcontinent region of North America, Ireland, Canada (Sverjensky, 1986; Leach and Sangster, 1993; Sangster, 1996, and reference therein). The principal challenge resides in interpreting the multiple generations of carbonate phases and their genetic link with the massive sulfide mineralization. Carbonate replacement facies and breccia cements are largely dominated by various episodes of early, and subsequent hydrothermal dolomitization, and calcite precipitation; whereas, silicate alteration includes authigenic clay minerals, feldspars, and a variable degree of silicification (quartz). Historically, much focus has been placed on characterizing dolomitization as it is coincident with a vast majority of Zn-Pb deposits in the Irish Midlands. Textural evidence presented herein may have implications in terms of ore-fluid physico-chemical properties (e.g. neutral pH of the ore forming fluid), and fundamental processes resulting in sulfide precipitation (e.g., Anderson, 1975; Anderson and Garven, 1987).

In general, silica and potassic alteration are recognized in Lower Paleozoic carbonate sequences hosting MVT Pb-Zn mineralization in the Eastern U.S.A., and Canada (Leach et al., 2010). Potassic alteration is marked by authigenic clay minerals (illite), and K-feldspar; whereas, silica alteration is reported as quartz and silicification. In the upper Mississippi Valley, thermodynamic modeling has suggested that  $a^{K^+}/a^{H^+}$  of ore forming fluids are consistent with a K-feldspar-muscovite-quartz assemblage (Barnes, 1979; Giordano, 1985; Giordano and Barnes, 1981). Potassic phyllosilicates ranging from illite to phengite are consistent with the presence of 2M<sub>1</sub>, 1Mt and 1Mc polytypes and illite crystallinity (Heyl et al., 1964). The occurrence of authigenic K-feldspar and illite in Appalachian limestones and sandstones are thought to be genetically related to occurrences of MVT mineralization (Hearn and Sutter, 1985; Hearn et al., 1987; Rothbard, 1983). These silicate mineral occurrences have been described in the historical Mississippi Valley area, but have been largely unresolved in other carbonate-hosted Zn-Pb deposits. These phases also have the potential to add geochemical and geochronological constraints on the mineralizing system, as they can be either authigenic, or reset by the hydrothermal fluids (e.g., Gays River and Polaris Zn-Pb deposits; Héroux et al., 2000; Kontak et al., 1994).

### 1.2. Barium and potassium feldspars in ore deposits

The first description of a Ba-bearing (barian) feldspar was that of hyalophane from alpine fissure-type veins in dolomite,

originally mistaken for adularia (Sartorius von Walterhausen, 1855). Barian feldspars (celcian and hyalophane) are typically restricted in occurrence, associated with exhalative hydrothermal processes, low to medium-grade metamorphism, and in volcanic or magmatic systems as a substitution in feldspar minerals (Gay and Roy, 1968; Smith and Brown, 1988; Deer et al., 2001, and references therein). According to Deer et al. (2001), the Ba concentration in feldspars is generally between 0.1 and 1.0 wt% (wt%) with rare occurrences exceeding 6 wt% BaO. The relative scarcity of barian feldspars resides in their formational environment rather than any difficulties in accommodating Ba<sup>2+</sup> into the mineral lattice; nevertheless, the genesis of barian feldspars remains poorly understood. The barian feldspar series is principally represented by celcian (Ba<sub>2</sub>Al<sub>2</sub>Si<sub>2</sub>O<sub>8</sub>) the Ba-end member, and hyalophane, (K<sub>1-x</sub>Ba<sub>x</sub>)Al(Si<sub>3-x</sub>Al<sub>x</sub>)O<sub>8</sub> (non-IMA mineral) the intermediate member of the celcian-orthoclase series, and both belong to the BaAl<sub>2</sub>Si<sub>2</sub>O<sub>8</sub>-KAlSi<sub>3</sub>O<sub>8</sub>-NaAlSi<sub>3</sub>O<sub>8</sub> ternary system. They are frequently identified in metamorphosed sedimentary exhalative (SEDEX)-type Pb-Zn (Cu) or Ba-Zn deposits, e.g. Kipasi, DRC; Broken Hill, NSW, Australia; Aberfeldy, Scotland, or Rozna in the Bohemian Massif of Czech Republic, Arrens in the French Massif Central (Chabu and Boulegue, 1992; Coats et al., 1980; Fortey and Beddoe-Stephens, 1982; Kribek et al., 1996; Moro et al., 2001; Pouit and Bois, 1986; Segnit, 1942), and also in barite deposits where feldspars may sequester Ba during metamorphism; similarly, barian feldspars can accommodate trace constituents in metamorphic environments, e.g., Mn in hyalophane from the Cuyuna Iron Range in Minnesota, U.S.A. (McSwiggen et al., 1994). For each of these instances, the barian feldspars are originating from the transformation (diagenesis and metamorphism) of barite or hydrated Ba-bearing silicates such as harmotome (Ba<sub>0.5</sub>Ca<sub>0.5</sub>KNa<sub>5</sub>Al<sub>5</sub>Si<sub>11</sub>-O<sub>32</sub>·12H<sub>2</sub>O) and cymerite (BaAl<sub>2</sub>Si<sub>2</sub>(O,OH)<sub>8</sub>·H<sub>2</sub>O).

By contrast, occurrences of potassium feldspar (adularia) in hydrothermal systems are far more common in alpine fissure-type, fluorite-barite, and low temperature polymetallic veins, high-sulfidation epithermal and porphyry systems as the result of widespread potassic, sericitic, and argillic alteration; its occurrence is largely dependent on temperature, pH, activity of K<sup>+</sup> and H<sup>+</sup>, and fluid-rock ratios (Dong and Morrison, 1995; Heald et al., 1987; Hemley, 1959; Marcoux et al., 1990; Seedorff et al., 2005). Lastly, Ba-bearing adularia have been described in the polymetallic vein deposits of Ain Barbar, Algeria, with BaO contents of approximately 4.8 wt% (Marignac, 1988). Interestingly, investigations of Ba-rich adularia (9.5 wt% BaO) from the Ouachita Mountains, Arkansas, U.S.A. have interpreted the authigenic feldspars as being genetically linked to post-collisional hydrothermal systems responsible for MVT (Pb-Zn-Ba) mineralization in northern Arkansas and southern Missouri, U.S.A. (Shelton et al., 1986).

### 1.3. The Rathdowney Trend in the context of the Irish ore field

Irish-type Zn-Pb (Ag) deposits along the Rathdowney Trend are hosted by variably dolomitized marine (reef) platform carbonates of the Waulsortian (see Philcox, 1984; Hitzman and Beaty, 1996). These Zn-Pb deposits are situated in the hanging wall of ENE-WSW normal faults, which developed during an extensional phase in the Early Carboniferous, resulting in an array of relay ramp dextral *trans*-tensional structures (Johnston et al., 1996). At the Lisheen and Galmoy deposits, major sulfide zones generally occur at the points of maximum throw along faults or as small ore bodies on secondary structures (Doyle and Bowden, 1995; Doyle et al., 1992; Shearley et al., 1992). A late phase of Variscan tectonic inversion post-dating the ores has also been documented (Johnston et al., 1996). These structures are thought to have facilitated the circulation of fluids deep into the basement, allowing for hydrothermal leaching, and transport of base metals (Wilkinson

et al., 2005a). Current metallogenic models developed for the formation of Zn-Pb deposits in the Irish Midlands (see Hitzman and Large (1986), Hitzman and Beaty (1996), Wilkinson (2003, 2010), Wilkinson and Hitzman (2015), and Johnston (1999) among others) involve the mixing of saline brines rich in bacteriogenic sulfur ( $\delta S^{34}$ -25 to -5‰) with a relatively high temperature moderately saline ore fluid (~12 wt% NaCl; up to ca. ~250 °C). Furthermore, alteration patterns of dolomitization, ore fluid compositions in relation to the formation of hydrothermal breccias and estimates from fluid inclusion studies have added considerable evidence for the current understanding of Irish-Type Zn-Pb deposits (Eyre, 1998; Fuscuardi et al., 2003; Hitzman et al., 2002; Redmond, 1997; Wilkinson et al., 2011, 2005b; Wilkinson and Earls, 2000).

Historically, the occurrence of barium feldspar in the Irish Midlands has been documented in the Silvermines District (Reed and Wallace, 2004), and at the Moyvoughly occurrence by Kucha (1988), but their composition, and placement in the paragenetic sequence relative to sulfide mineralization is still unresolved. Similarly, white micas and hydrothermal illite have been noted in altered ORS beneath Irish-type Zn-Pb mineralization (Mallon, 1997), as well as in the host carbonate sequence; although noted as a minor constituent of the sulfide paragenesis (Hitzman and Beaty, 1996; Wilkinson et al., 2011), illites are not fully constrained. On the basis of the lithochemical constraints provided by Wilkinson et al. (2011), the authors indicate an overall gain in K within ore sulfides and host breccias and a possible association of Ba with the feeder zones; however, a the paucity of Si analyses in

bulk lithochemical data for the Irish Midlands limits characterization of authigenic silicate phases.

The objectives of this work are to (1) characterize the mineralogy of potassic alteration in relation to base-metal (sphalerite) mineralization, (2) develop a novel approach for the quantitative study of breccias integrating the textural and chemical aspects, (3) interpret ore textures and the mineralogical assemblages in terms of ore forming processes, and (4) place additional constraints on the ore stage mineralization as it relates to alteration facies.

## 2. Sampling and methodology

A total of 29 samples from eight drillholes along the Rathdowney Trend were collected to provide a representative set of black matrix, and white matrix breccias, fault gouge, and massive sulfide mineralization. Respectively from the WSW to the ENE, samples were collected from the Main Zone including the Oolite Zone, the Island Zone, as well as the Rapla prospect 20 km to the NE, near the former Galmoy Zn-Pb Mine (Fig. 1 and Table 1).

Scanning electron imaging and quantitative chemical analyses were carried out on minerals using a Tescan Mira field emission gun scanning electron microscope (FEG-SEM) equipped with an Oxford X-Max<sup>N</sup> 150 mm<sup>2</sup> energy dispersive spectrometer (EDS). Elements were calibrated on natural standards (augite, anorthoclase, microcline, olivine, rutile, pyrite), metals (Cu, Sb, Pb, Zn), and synthetic standards (InAs, PbTe). Silicate standards were provided by the Smithsonian Institute Department of Mineral Sciences. The acceleration voltage and beam current were set at

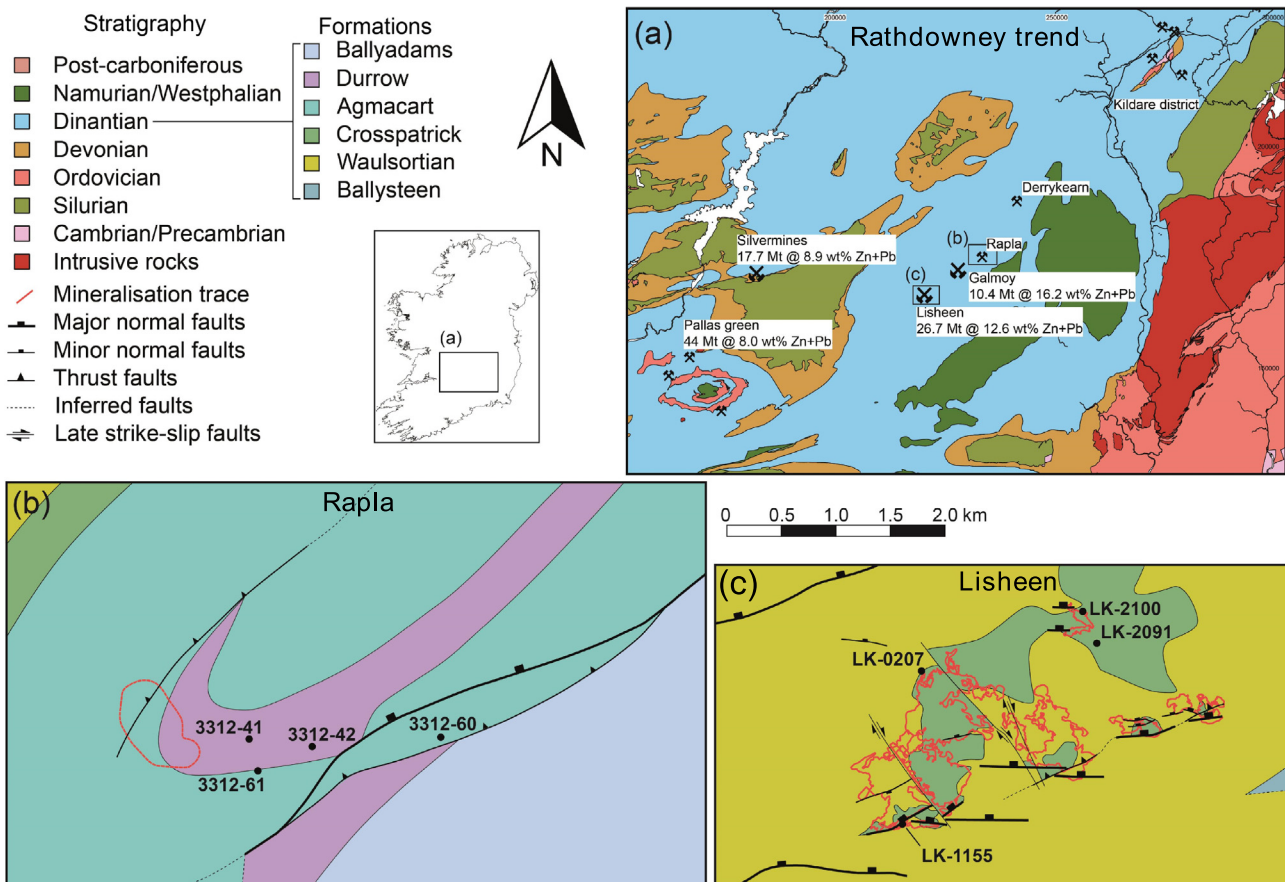


**Fig. 1.** Simplified geological map of the Lisheen Rathdowney trend map (a). Sampled drillhole locations reported on the detailed map for Rapla (b) and Lisheen (c). Main Zone: LK-1155 and LK-0207, Island: LK-2100 and LK-2091, Rapla prospect: 3312-41, 42, 60 and 61, noted as Rxx in the sample list. Compilation of mineral resources and past production and outline of the ore bodies from Kyne et al. (2017) and Turner et al. (2016).

**Table 1**  
Sample location and depths for the Lisheen deposit and Rapla occurrence.

Drillhole	Sample depth (meter)	Area	Description
LK1155	146.7, 147.0, 165.5, 169.3, 169.15, 169.30	Main Zone	Massive sulfide mineralization
LK207	148.5, 150.1, 184.6, 192.0	"	Black matrix breccia
LK2100	240.5, 248.8, 258.3, 258.4, 255.9	Island	Sulfide mineralization and black matrix breccia
LK2091	244.3, 244.35	"	Black matrix breccia
R41	651.9	Rapla	Clay gouge
R42	590.4, 591.6, 598.0, 602.0, 602.5, 611.7, 636.5, 651.8	"	Stylolithes, microbreccia with variable and weak sulfide mineralization
R60	180.7	"	
R61	532.5, 623.7	"	

15 kV and 0.3 nA for the silicate analysis (Si, Al, Ca, Na, K, Mg, Ti, Ba), and at 20 kV and 0.25 nA for sulfide analysis (S, Fe, Cu, Zn, Pb, As, Cd). The live counting time was set at 60 s in both experiments, while analytical conditions maintained the EDS detector dead-time at approximately 30%. The detection limits are below 0.1%. Semi-quantitative chemical maps were obtained by producing a montage of individual X-ray maps.

Image processing and analysis were performed using Image J software (Schneider et al., 2012). Fractal analysis of clast morphologies were performed using the Euclidian Distance Mapping (EDM) methodology and Image J macro developed by Bérubé and Jébrak (1999). The novelty resides in the definition of the fragments based on the large-scale mapping capabilities of the SEM to define and extract the boundary of elements using the chemical maps.

Clay mineral separates were obtained through sample pulverization in a ceramic mortar, followed by ultrasonic dispersion in deionized water. The infra 5  $\mu\text{m}$  fractions extracted, were characterized using X-ray diffraction on dried clay mineral separates using a Siemens D5000 diffractometer on oriented and randomly oriented mounts. The samples were analyzed with  $2\theta$  ranging from 2 to 30° for oriented slides (on a low background Si wafer), and a  $2\theta$  of 19–34° for determination of polytypes, with a step size 0.01°  $2\theta$  step, and a counting time per step of respectively, 1 and 5 s. The tube current and voltage were set at 40 mW and 40 kV, respectively.

### 3. Petrography and paragenetic association of the alteration with the base metal mineralization

Ore textures are quite varied and complex ranging from colloform replacements in breccia zones (Fig. 2A), as colloform ribbons of dark brown to pale yellow “honey-blende” sphalerite surrounding dolomitic clasts, to semi-massive to massive fine-grained mineralization almost solely composed of sphalerite with a distinct metallic grey color (Fig. 2B and C). The mineralization shows variable, complex association with the gangue sulfides (pyrite-arsenian pyrite), as well as breccias (Fig. 2D and E). However, a similar paragenetic association of sphalerite replacement of pyrite can be observed in the studied samples from both Main and Island Zones.

#### 3.1. Mineralogy of the Lisheen Main Zone

Macroscopically, sulfides are best described as massive with replacement textures of pyrite as well as replacement of clasts within the polygenic black matrix of the breccias. Intercalated sedimentary material is not uncommon, mainly represented by fine laminae of gangue carbonates with disseminated sulfides. Fragments (clasts) of mineralization are also found in the breccias hosted by late euhedral calcite veins cross cutting the ore zones. The sulfides consist of sphalerite and galena with variably abundant pyrite with variable As content, and minor marcasite.

Non-sulfide gangue minerals are composed of dolomite, calcite, euhedral quartz, illite, apatite, and large idiomorphic or neoformed (as pore-filling) barian (Ba, K) feldspar. The relative proportion of carbonates to silicates can be quite variable and the barian feldspar appears to occupy a large volume of the rock (Fig. 3A and B). The barian feldspars are accompanied by adularia and albite forming large (up to 100  $\mu\text{m}$ ) euhedral to sub-euhedral rhombic crystals, arranged in blocky masses co-genetic with large zones of sphalerite (Fig. 3A–C). These feldspars appear to be entirely neoformed and no detrital cores with secondary overgrowths were encountered. Minor illitization of the feldspar is present, and most of the phyllosilicates can be identified as sericite or illite depending on their morphologies. Sericite is found as flaky or sub-idiomorphic habits (10–30  $\mu\text{m}$ ), whereas illite forms minute aggregates of laths and needles (5–15  $\mu\text{m}$  in length) or overgrowths on preexisting sericite; both are present in the intergranular porosity, as neoformed phases (Fig. 3D–F). Illite is also present as spherules and laths, both habits co-genetic with a phase of sphalerite precipitation (Fig. 3D–F). It can be noted that illite is generally only present with sphalerite and no illite was identified in the early gangue sulfide phases. These gangue sulfides consist of an early arsenian pyrite followed by at least two generations of pyrite. In the Lisheen Main Zone, the first generation of pyrite is present as an early sub-idiomorphic form (pyrite I), followed by an overgrowth of pyrite of a less distinct morphology largely replaced by sphalerite in the form of diffuse spherulites.

#### 3.2. The Island Ore Zone

In contrast to the Main Zone, barian feldspars were not identified in thin sections from the Island Ore Zone. However, illite is found in association with various facies of sphalerite (large masses, colloform), in places forming reaction rims around euhedral quartz crystals. The paragenetic sequence for pyrite at the Island Ore Zone is as follows: an early euhedral arsenian pyrite (I) followed by pyrite (II) overgrowths with pervasive sphalerite replacement partially masking earlier textures, a third generation of pyrite (III) comprising idiomorphic crystals that post-date Zn-Pb mineralization, and a late framboidal pyrite (IV) forming in the intergranular porosity of late- to post-ore breccias zones (Fig. 4A). It is important to note that pyrite (II) is preferentially replaced by sphalerite, while the arsenian pyrite (I) is more frequently partially preserved (Fig. 4B). Relative to the sulfide paragenesis, idiomorphic quartz is crystallizing syn- to late pyrite (I), and is co-genetic with colloform sphalerite. This assemblage is filling small (1–5 mm) vugs in dolomite, but disequilibrium textures such as corrosion and (or) replacement of dolomite are not systematic. Evidence of reaction textures and disequilibrium are, however present in sphalerite, where the co-genetic illite is growing at the expense of euhedral quartz forming rims or aggregates of thin laths (Fig. 4B–D). Minute crystals (<10  $\mu\text{m}$ ) of sub-euhedral apatite are also present in these illite reaction rims (Fig. 4D). These large areas of massive sphalerite are optically continuous without, rims, bands, or evidence of zona-

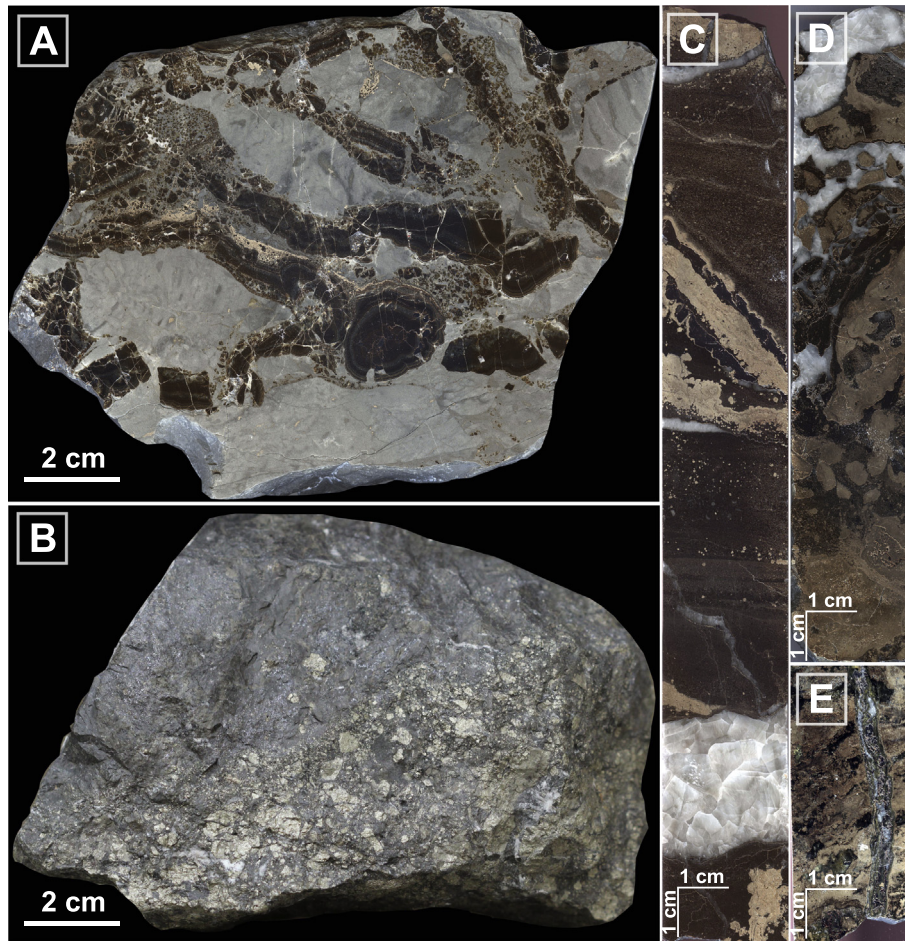


**Fig. 2.** Ore textures from the Lisheen mine area. A) Colloform sphaerite in vugs, the ribbon textures fills the matrix of a brecciated dolomitic limestone. The clasts show minor sulfides, mainly pyrite associated with millimetric development of proto black matrix breccias. B) Massive sphaerite mineralization with minor galena cementing pyrite fragments. C) Disseminated sulfide mineralization and cross cutting calcite veins, D) Mineralized clasts in black matrix breccias and partial replacement of internal sediments or black matrix breccias by sphaerite and pyrite E) Potassic silicate-bearing massive sulfide mineralization. Late calcite veins and veinlets cross cutting the ore are unrelated to mineralizing events.

tion. Additionally, colloform varieties of sphaerite show alternating bands of dark brown to pale yellow (honeyblende) sphaerite with hematite inclusions; sphaerite is also found as isolated ribbons dismembered and cemented by euhedral pyrite (III) in the dolomitic matrix or in concentric vug-fills, growing around euhedral quartz crystals (Fig. 4E and F). The protobreccia and cataclastic textures with fragments of banded sphaerite and laths of illite may be seen as immature black matrix breccias (Fig. 4G and H). The presence of disseminated sphaerite clasts as well as rim overgrowths, with laths of illite filling the matrix and cementing the dolomite fragments (Fig. 4H) exemplifies the protracted formation of the breccias during the mineralization events.

### 3.3. The Rapla Zn-Pb occurrence

The Rapla Zn-Pb occurrence allows for the investigation of mineralogical changes related to the fluid-rock interaction potentially more distally to the main ore zones of Lisheen and Galmoy. In addition, the faulted contact between the Waulsortian reef limestone and argillaceous limestones of the Ballysteen Formation is preserved at Rapla, allowing for investigation of clay-rich gouge. This contact is underlined by a fracturation corridor with intercalations of deci-centimetric clay gouge, where the dislocated rock is surrounded by a matrix composed of clay and milled wall rock

(dolomite). At the microscopic scale, similar textural relationships are observed (Fig. 5A). Pre-existing discontinuities such as stylolite joints have been reactivated and are sites of preferential development of micro-breccia textures, with minor sulfide precipitation (Fig. 5B). These areas display textures indicative of dissolution recrystallisation of the detrital micas marked with Ti exsolution and reprecipitation of titanium oxides, and multiple chemically variable (As-rich bands) overgrowths on the idiomorphic diagenetic pyrite (Fig. 5C and D).

### 3.4. Black matrix breccias and hydrothermal phyllosilicates

In an attempt to link paragenetic and petrographic observations at larger scales ( $10 \times 10$  mm or larger), X-ray element maps were produced to investigate the relationships between fragments and the very fine-grained matrix of the breccias, which is indistinguishable macroscopically and in backscattered electron images (Fig. 6A and B). Such maps can be used to explore the mineralogy of the fragments, their relative proportions, morphologies and relationship to the matrix. This use of chemical mapping also represents a new approach for the textural study of breccia bodies, allowing for the extraction of fractal dimensions of particle morphology ( $D_r$ ) and particle size distribution (PSD), both linked to the genetic processes of the breccias (Blenkinsop, 1991; Jébrak,

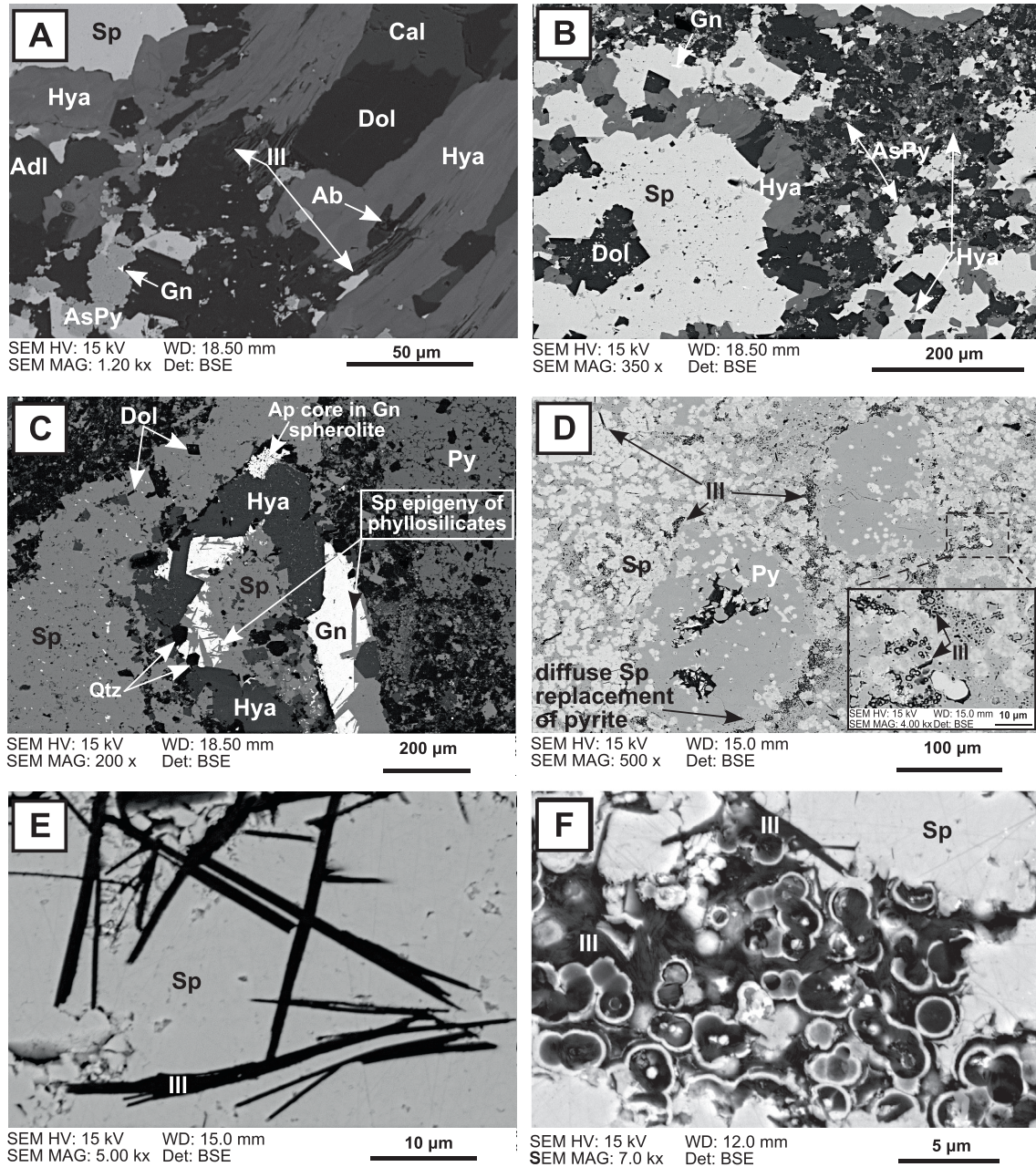


**Fig. 3.** Ore and gangue petrography of the Lisheen Main Zone ore body. A) Main Zone ore with (K, Ba) feldspar, minor adularia and albite, all cogenetic with sphalerite. Minor illitization is present on the edges of crystals. B) Hyalophane-rich gangue associated with sphalerite. The (K, Ba) feldspars form sub-euhedral to euhedral crystals and are significantly more abundant than carbonates. C) Sphalerite, galena, hyalophane, quartz and dolomite assemblage, minor apatite in the core of galena spherulites D) Replacement texture of pyrite by sphalerite and an aggregate of illite laths. E) Illite laths in massive sphalerite. F) Spherulite of illite with sphalerite rims in an illite aggregate. Abbreviations listed as follows, Cal: calcite, Dol: dolomite, Qtz: quartz, Ap: apatite, Ab: albite, Adl: adularia, Hya: hyalophane, Ill: illite, Sp: sphalerite, Gn: galena, AsPy: arsenian pyrite.

1997). In the present study, we focused on the fragment geometry due to the difficulties of image processing to extract and count the fragments accurately.

Within the black matrix breccias, the proportion of fragments and matrix are quite variable ranging from clast supported to matrix supported with a high proportion of matrix, overall. The mineral proportions computed from X-ray element mapping are 61% dolomitic fragments, 27% matrix, 4% sulfides (dominantly pyrite with minor sphalerite), and 1% quartz; 7% of the examined section remains non-classified (e.g. composite pixels, micro-porosity). The X-ray element maps reveal that the matrix composition is dominated by Si, Al, and K, in agreement with the illite neofor-

mation observed elsewhere and intimately cemented by recrystallized dolomite at a micro-scale (Fig. 6A and B). The fractal dimension of the fragment morphologies ( $D_f$ ) is indicative of their rough anhedral nature, with increasing  $D_f$  values reflecting an increase in shape complexity. For example,  $D_f$  values of less than 1.1 are considered 'low', between 1.1 and 1.2 'medium', and  $D_f$  values above 1.2 'high' (Jébrak, 1997). The values computed for the black matrix breccia fragments extracted from X-ray element maps for the Island Ore Zone range from 1.15 to 1.34, with an average value of 1.29 ( $\sigma = 0.09$ ). The values for the Main Zone black matrix breccia fragments, computed from photography, range from 1.08 to 1.15 with an average value of 1.11 ( $\sigma = 0.03$ ), (Fig. 6C). Lower

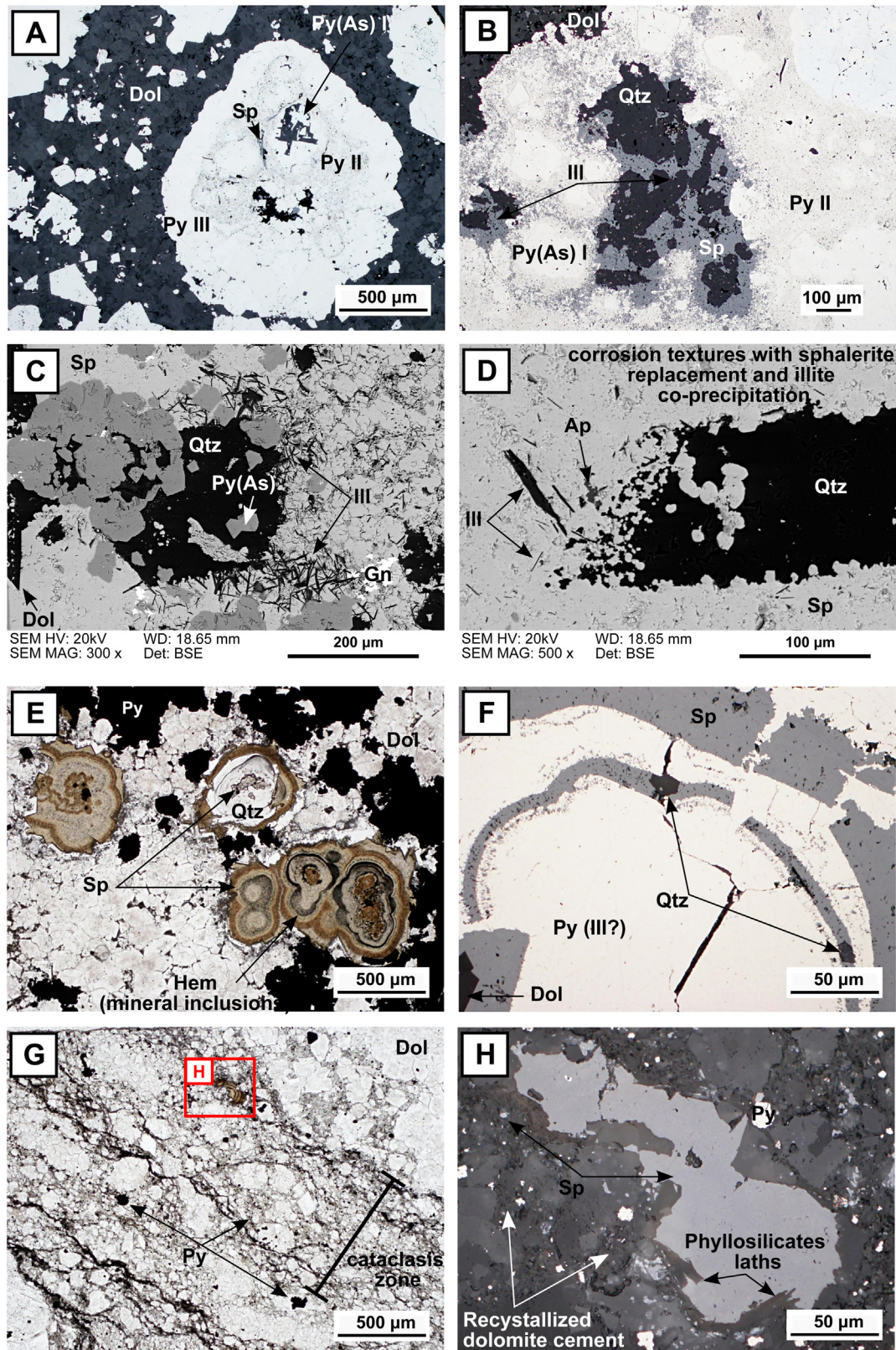


**Fig. 4.** Ore and gangue petrography of the Lisheen Island Zone ore body, featuring the hydrothermal clay mineral morphology. A) Multiple pyrite generations with spherulitic replacement, showing preferential pyrite overgrowth around arsenian pyrite. Late idiomorphic pyrite post-dates the mineralization. B) Quartz dissolution with corrosion textures (ragged edge, embayments) and pyrite (II) replacement during spherulitic and illite co-precipitation. C) Euhedral quartz with idiomorphic arsenian pyrite inclusions showing reaction rim with illite lath neof ormation in the quartz corrosion zones associated with spherulitic. Late galena is filling the remnant intergranular porosity. D) Progressive quartz corrosion associated with illite, apatite co-precipitation with spherulitic. E) Spherulitic inclusions in sub-euhedral quartz surrounded by a rim of quartz overgrowth followed by ribbons of collomorph spherulitic. The spherulitic ribbons can show inclusions of minute lath shaped crystals of brownish red color, possibly specular hematite. F) Euhedral quartz within banded spherulitic. G) Cataclasis zone, forming a proto black matrix breccias with a clay and recrystallized dolomite cement. H) Detailed view of a banded spherulitic clast with illite lath in a microbreccia.

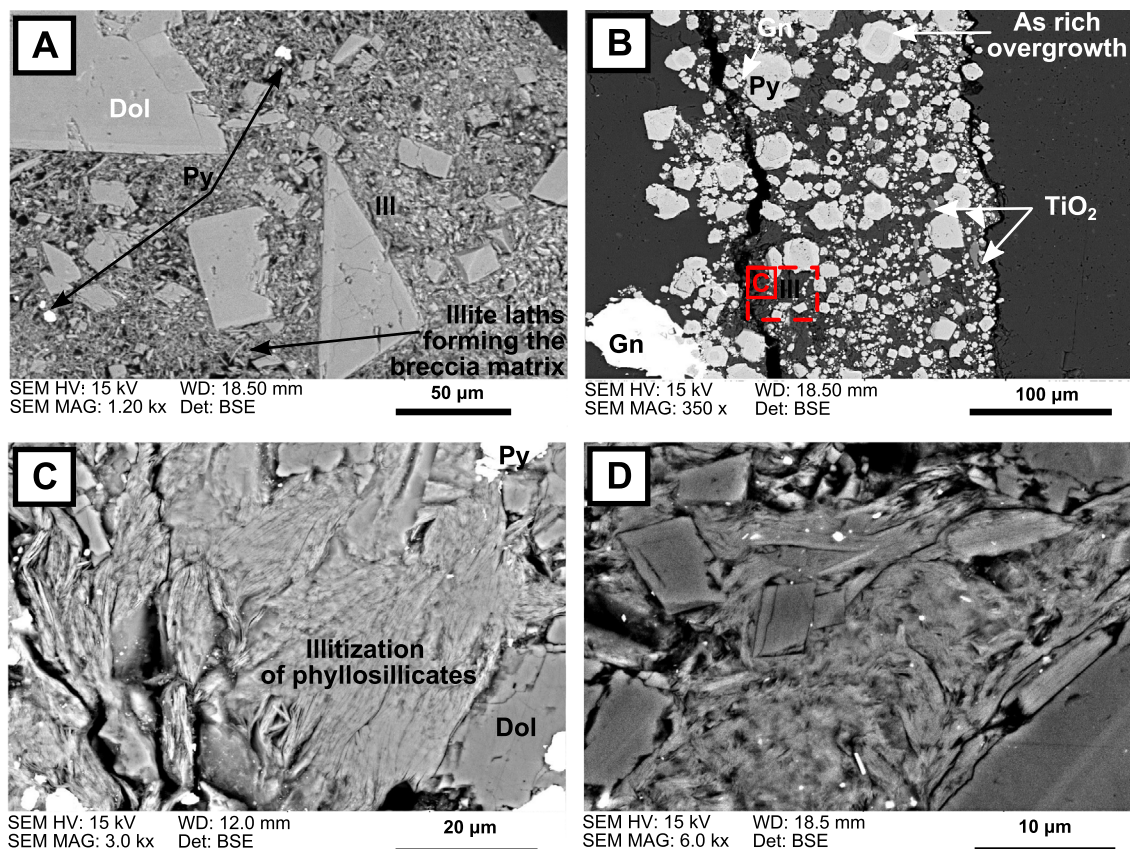


**Fig. 5.** Fault gouge and proto breccias in the Rapla prospect. A) Illitic fault gouge with floating clasts of broken dolomite at the contact between the Waulsortian dolomitic limestone and the argillaceous bioclastic limestone of the Ballysteen Formation (ABL). B) Protobreccia developed on a stylolitic joint with numerous titanium oxides, possibly anatase, and minor late galena. C) Recrystallisation of illite lath on micas and chlorites. D) Illitic microfault zone formed of intricate laths of neofomed illite developed from the alteration of micas.

values computed from photography could be attributed to difficulties in extracting shapes when very low contrast of colors or levels of grey exists between the fragments and the matrix. Furthermore, large less-altered clasts were selected on the basis of photography, as their contours were progressively fading with the matrix for the most altered clasts. This enhanced the success of the element mapping technique, overcoming the clast shape definition and extraction issues in the analytical procedure. Finally, the high fractal  $D_f$  values are interpreted to be the result of chemical corrosion (Jébrak, 1997). This is supported by the diffuse boundaries of some clasts that are progressively detached from larger fragments indicating chemical corrosion as a prominent process in the formation of the black matrix breccias.

#### 4. Crystallochemistry of gangue minerals

##### 4.1. Feldspar chemistry

In a celsian-orthoclase-albite plot (Cn-Or-Ab), feldspars from Lisheen are seen to be largely represented by a barian (Ba,K) composition, with minor adularia, and albite (Fig. 7). The barian feldspar composition falls between  $Cn_{32-40}$ , consistent with the mineral hyalophane (Table 2). Hyalophane compositions are usually within-but not restricted to a range of 5–30 mol% Cn. The compositions obtained for the feldspars in the Lisheen Main Zone are relatively homogeneous. Subtle zonation is thought to reflect minor variations in the Ba/K ratio and can, in places be identified in backscatter electron images; the primary substitution being between Ba-Al and K-Si (Gay and Roy, 1968). Adularia and albite

crystals present are close to the theoretical end-members for these minerals and generally contain less than half a weight percent (wt %) BaO; only one adularia analysis exceeded these limits providing a value of 1.16 wt% BaO. Contents of Mg, Mn, Ti, and Fe are close or below the detection limit. Comparison with historical data is difficult as this data represents the only compositions reported on such feldspars for the Rathdowney Trend. However, the compositions are broadly comparable with those reported for the north Midlands (Moyvoughly prospect) by Kucha (1988). The presence of hydrothermal barian feldspar likely results from hydrothermal processes, for which barium is preferentially integrated into the silicate network rather than in sulfates or carbonates. In a saline ore bearing solution (see Wilkinson et al., 2005a), transport of the divalent hydrated  $Ba^{2+}$  ion would be enhanced by the barium chloride complex (Hanor, 2000). The reaction between dissolved  $Ba^{2+}$  and  $SO_4^{2-}$  should produce precipitates of very low solubility; the paucity of barite and anhydrite would suggest a deficiency of dissolved sulfate in the hydrothermal fluids. Therefore, reducing conditions may persist at the site of ore deposition, where reduced sulfide anion complexes predominate over sulfate, hindering the precipitation of barite.

##### 4.2. Phyllosilicate minerals

Intimate textural relationships between minute (<1  $\mu$ m thick) lath or needle-like phyllosilicate minerals and their encapsulating host phases (sphalerite, quartz and carbonates) makes in situ analysis particularly challenging. Increases in Si, Ca and Fe may be due to possible contamination from other minerals, a result of



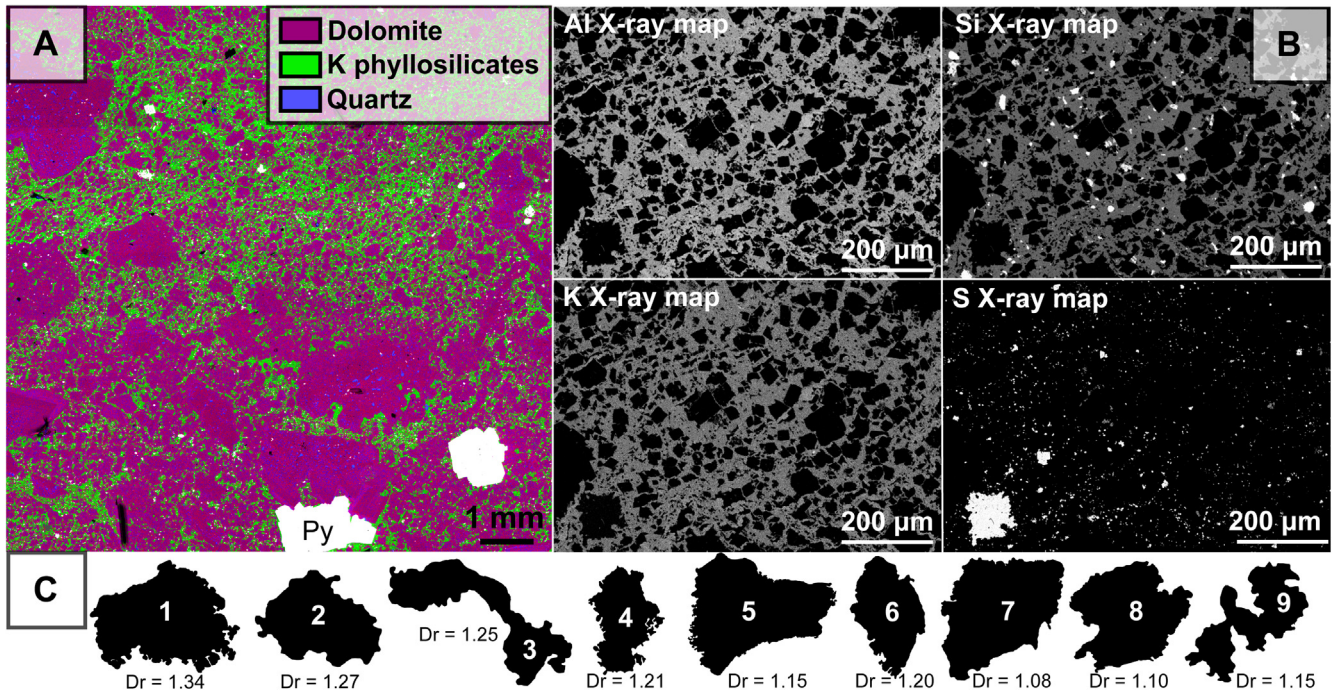


**Fig. 6.** A) Composite image of an X-ray semi-quantitative chemical map of the black matrix breccias for Si, K, Al, Ca, Mg, Fe, Zn, and S. B) High resolution Al, Si, K and S X-ray chemical maps over the same area of matrix selected from Fig. 6A. The maps are illustrating the abundance of potassic phyllosilicates in the matrix. The sulfur map reveals both pyrite (bright white) and sphalerite (darker levels of grey) disseminated in the matrix. C) Fragments used for the computing of the fractal dimension of the morphology of particles ( $D_r$ ) using Euclidian Distance Mapping (EDM). The fragments (1–6) are from Island and extracted from the chemical map and fragments (7–9) from the Main Zone ore body were extracted from a photograph.

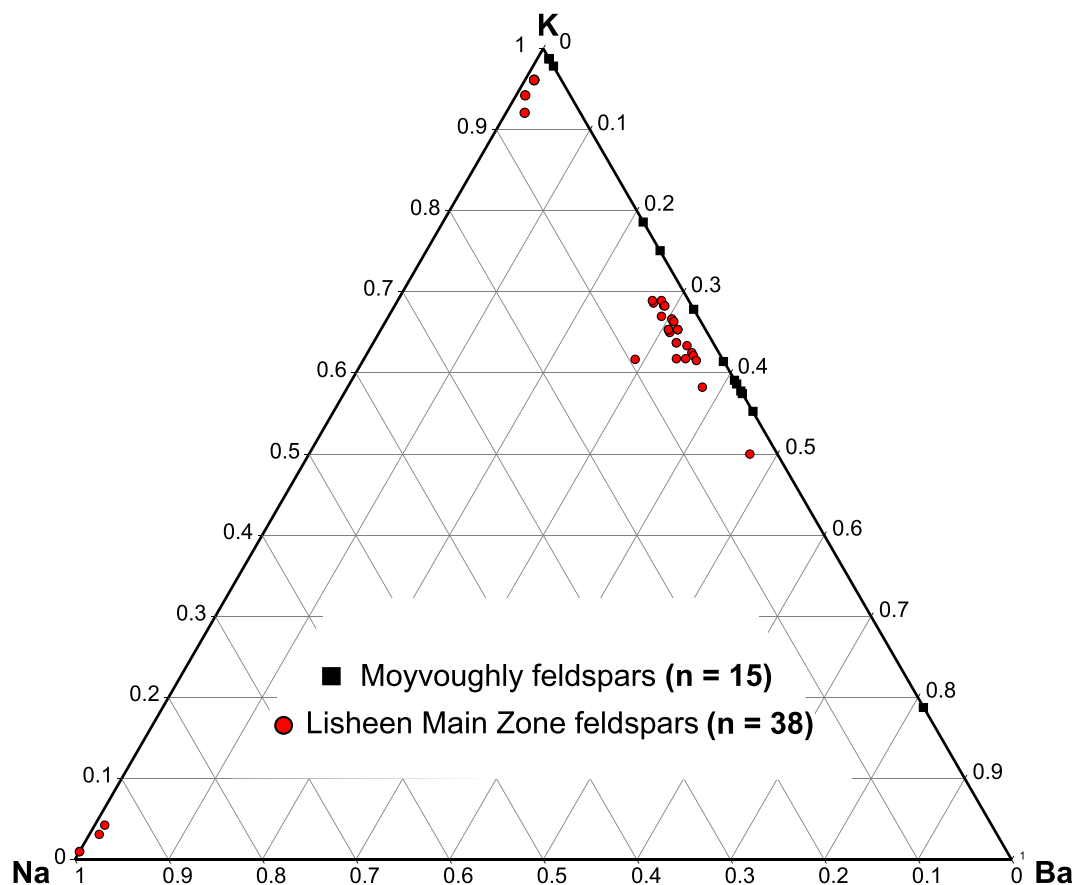


**Fig. 7.** Ternary (Cn-Or-Ab) diagram of the feldspar composition from the Lisheen mine (solid circle) round, and data, from Kucha (1988) (solid square), in atom per formula unit (apfu). It must be noted that sodium was not analysed by Kucha (1988).

**Table 2**

Representative chemical analysis on feldspar and phyllosilicates. The structural formulas are respectively based on 8 and 11 oxygens normalizations.

	Adularia	Albite	Hyalophane		Illite/phengite			
SiO <sub>2</sub>	64.52	67.21	54.10		1	2	3	4
TiO <sub>2</sub>	0.00	0.00	0.00	Si	3.23	3.50	3.49	3.19
Al <sub>2</sub> O <sub>3</sub>	18.38	19.65	20.94	Al <sup>IV</sup>	0.77	0.50	0.51	0.81
FeO	0.12	0.17	0.06					
MnO	0.05	0.03	0.01	Al <sup>VI</sup>	1.79	1.60	1.52	1.74
MgO	0.02	0.08	0.05	Fe <sup>2+</sup>	0.08	0.08	0.07	0.09
CaO	0.06	0.17	0.10	Mg	0.13	0.33	0.42	0.13
Na <sub>2</sub> O	0.32	10.69	0.40	Ti	0.01	0.01	0.02	0.03
K <sub>2</sub> O	16.84	0.54	10.99	Mn	0.00	0.00	0.00	0.00
BaO	0.42	0.61	13.98					
Sum	100.73	99.12	100.48	Oct	2.01	2.02	2.03	2.00
<i>Number of ions</i>								
Si	2.98	2.98	2.74	Ca	0.00	0.04	0.05	0.01
Al	1.00	1.03	1.25	Na	0.08	0.01	0.02	0.12
Fe	0.00	0.01	0.00	K	0.85	0.76	0.78	0.87
Ti	0.00	0.00	0.00					
Mg	0.00	0.01	0.00	1 Main Zone				
Mn	0.00	0.00	0.00	2 Island				
Na	0.03	0.92	0.04	3 BMB corridor SW of the Island				
Ca	0.00	0.01	0.01	4 Rapla				
K	0.99	0.03	0.71					
Ba	0.01	0.01	0.28	Oct: sum of octahedral ions				

the X-ray emitting volume generated by the electron beam. Barium was not detected with the operating conditions used for in-situ analyses, and can be considered negligible in phyllosilicate phases.

The potassic phyllosilicate compositions reported (Table 2) are in agreement with the general structural formulae of micas (muscovite/sericite, and phengite) and illite (interlayer charge, octahedral occupancy, water content). According to the IMA report on the nomenclature of micas (Rieder et al., 1998), dioctahedral minerals with a total interlayer cation per half unit cell comprising between 0.6 and 0.85, and 0.85 to 1.0, should be termed illite and micas (muscovite or phengite), respectively. However, as noted by many authors, this definition of micas also includes the apparent end-member of the illite series, and muscovite is not stable with respect to illite (e.g. (Meunier and Velde, 2004; Rosenberg, 2002), and references therein). A more rigorous definition would entail a charge equal to 1 for muscovite or phengite when the Tschermak substitution is present; while a charge of 0.9–0.75 would represent illite, with the high charge illite (0.87–0.90) often being of the 2M1 polytype.

In the Rathdowney Trend, the field of composition for micas in a MR<sup>3</sup>-2R<sup>3</sup>-3R<sup>2</sup> ternary diagram indicates a distribution along the muscovite-phengite line, in the field of composition attributed to dioctahedral micas (Fig. 8). This is consistent with the Tschermak substitution for white micas with R<sup>2+</sup>(VI) + Si<sup>4+</sup>(IV) = Al<sup>3+</sup>(VI) + Al<sup>3+</sup>(IV), with R<sup>2+</sup>(VI) = Mg<sup>2+</sup> + Fe<sup>2+</sup>, as shown by the linear relation between on the Si<sup>4+</sup> vs R<sup>2+</sup> plot, (Fig. 8). In addition, the binary plot of Si versus the interlayer charge allows us to distinguish two groups of minerals, also confirmed petrographically (Fig. 8). The first group, with a high interlayer charge between 0.9 and 1.0 can be attributed to large sub-idiomorphic sericite and large illite laths. The second, with an interlayer charge 0.75–0.85 can be associated with the minute lath shaped forms, as isolated crystals, in aggregates or as overgrowths on sericite. Such an interlayer charge is consistent with the crystallochemical properties used to define illite (Meunier and Velde, 2004). Analyses with interlayer charges higher than 1 are systematically associated with high potassium (0.94–0.99 K<sub>(afpu)</sub>) and sodium (0.1–0.14 Na<sub>(afpu)</sub>). This could be attributed to the analytical error margin, but are likely an indication of crystallization at higher temperatures.

Classification of phyllosilicates is not always possible and it appears that the petrographically identified lath shaped illites are closer to the mica, phengite end-member. This exemplifies the dif-

iculties with classification of the high charge dioctahedral phyllosilicates. In fact, the high charge illites represented by the 2M<sub>1</sub> polytype are only observed for charges from 0.87 to 0.9. Meunier and Velde (1989) showed that the composition domains for the different micas and illite polytypes (2M<sub>1</sub>, and 1 M) could be distinguished in a M<sup>+</sup>-4Si-R<sup>2+</sup> plot. Then, using this projection the data from the Lisheen district, can be distributed along the phengitic line, indicating a dominance of phengite and of the illite 2M<sub>1</sub> polytype, while the trend of data toward lower potassium values marks the development of 1 M illite (Fig. 8). This is also in agreement with the petrographic observations of both sub-idiomorphic sericite (phengite) and the laths of illite.

The limited X-ray diffraction (XRD) data also suggests that the phyllosilicates are illitic in nature; however, issues in the clay extraction (separation and concentration) from the host rock did not always provide sufficient material for adequate XRD acquisition. Randomly oriented powder mounts from the fault gouge display a mix of 2M<sub>1</sub>, 1M<sub>cis</sub>, and 1M<sub>trans</sub> polytypes. This is in agreement with the textural observations showing replacement of detrital micas and (or) hydrothermal sericite/phengites by lath or needle shaped illite.

## 5. Discussion

One of the main challenges encountered during the exploration for carbonate hosted Zn-Pb deposits is the relative paucity of distinct hydrothermal alteration halos. Although significant progress has been made to better understand the reservoir properties, the nature of ore-bearing fluids (salinity, temperature, pH and δ<sup>34</sup>S), and structural controls on the setting of sulfides in the Irish Midlands, distinct geochemical or mineralogical pathfinders for the mineralization require improvement in the search for new resources. Recent studies have identified geochemical zoning (proximal-distal) related to hydrothermal feeder zones for the Lisheen deposit revealing a net gain in Li, K, Be, V, Ba and P in black matrix breccias (Fusciardi et al., 2003; Wilkinson et al., 2011). Historically, efforts were largely focused on complex successions of altered carbonates while a complete paragenesis of hydrothermal gangue minerals was not fully resolved. Integrating petrological research on silicate gangue minerals with established thermodynamic constraints for classic MVT and Irish carbonate-hosted

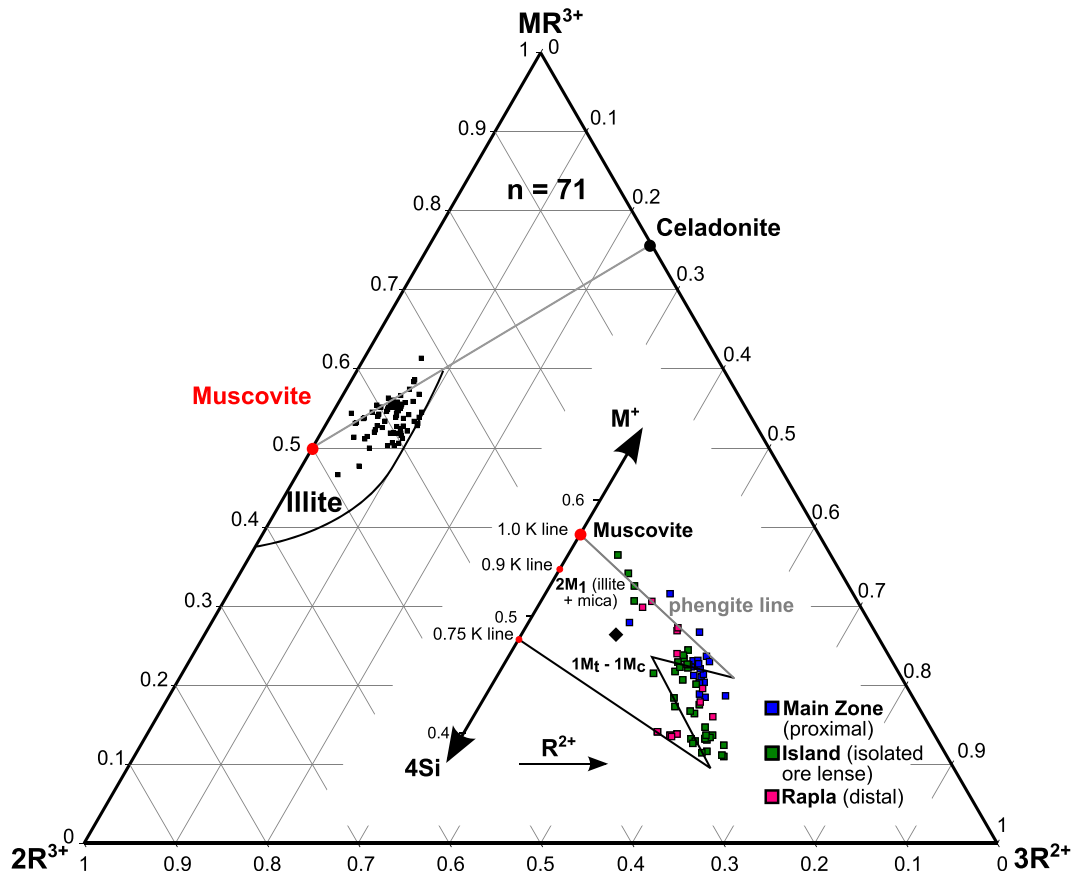


Fig. 8. Chemical composition and of illite and phengite from the Lisheen and Rapla ore zones plotted in the  $MR_3-2R_3-3R_2$  and  $M^+-4Si-R_2^+$  coordinates.

Zn-Pb systems will contribute to a better understanding of fluid rock interactions during hydrothermal processes (Fig. 9).

#### 5.1. Potassic alteration in the Irish Midlands vs other carbonate hosted base metal ore deposits

Far from being an isolated mineralogical oddity, the occurrence of silicate minerals in Lower Carboniferous limestones of the Irish Midlands seem to be in fact, relatively common. Occurrences of feldspar and phyllosilicate minerals have been noted by Mallon (1997) as a possible hydrothermal overprint observed in the Old Red Sandstone in the vicinity of deposits, as well as in the central midlands basin by Reed and Wallace (2004) at Silvermines, and at the Moyvoughly prospect (Navan Group) (Kucha, 1988), and in the Rathdowney Trend (current study). In contrast, occurrences of hydrothermal feldspars and phyllosilicates and their partially zoned distribution (distal-proximal) around orebodies have been identified for numerous MVT deposits in the U.S.A. (Heyl et al., 1964; Stormo and Sverjensky, 1983) while a co-genetic link has been discussed between brine migration in the carbonate strata and the occurrence of authigenic feldspars during ore deposition for MVT systems (Leach and Rowan, 1986; Shelton et al., 1986). Apart from mineral identification, the lack of research focus on these silicate and phosphate gangue phases has meant that their integration into the sulfide paragenesis or the whole rock geochemistry has not been fully considered; despite fluid inclusion analyses for the Irish Midlands having high potassium (from 1000 up to 35,000 ppm), and barium (900 ppm) concentrations (Banks et al., 2002; Johnson et al., 2009; Wilkinson et al., 2005a). Moreover, the Eu anomaly associated with the addition of Ba iden-

tified by Wilkinson et al. (2011) is interpreted as a higher temperature and reduced fluid signature, conditions required to efficiently mobilize  $Eu^{2+}$  (Sverjensky, 1984). This is in good agreement with the integration of barium in the crystal structure of silicates in a predominantly reduced environment. It also indicates that barium is not exclusively deposited as barite and could reflect the degree of mixing between seawater-derived fluids (sulfur source) with hydrothermal fluids ascending along faults. The precipitation of hydrothermal feldspars may indicate a dominance of the hydrothermal fluid over the basal brine, marking a significant hydrothermal pulse, while the same fluid on its migration path within the carbonate sequence would precipitate barite when oxidized sulfate becomes more abundant. Finally, the experimental determination of the field of stability for feldspars, indicates a dominance of adularia over albite. The presence of adularia and minor albite would suggest a higher sodium content in the fluid (Hemley and Jones, 1964), which is in agreement with current ore models (based on fluid inclusion data) requiring a saline metal-bearing brine e.g. (Wilkinson et al., 2005a).

A similar assemblage of K-feldspar  $\pm$  illite  $\pm$  quartz is present, and associated with a noted increase of the ratio of the 2 M polytypes for illite toward the ore zone (Heyl et al., 1964), which could in fact mark a predominance of phengite. Additionally, the K-feldspar-muscovite-quartz assemblage has been used by many authors to constrain the activity of potassium ion to hydrogen ion ( $a_K/a_{H^+}$ ) in the ore forming fluids (Barnes, 1979; Giordano and Barnes, 1981). Also, phengite is thought to form in response to a change in the temperature-dependent  $H^+$ /alkali ratio in a water rock system (Hemley, 1959; Meunier and Velde, 1982). Consequently, the development of illite or phengite rather than

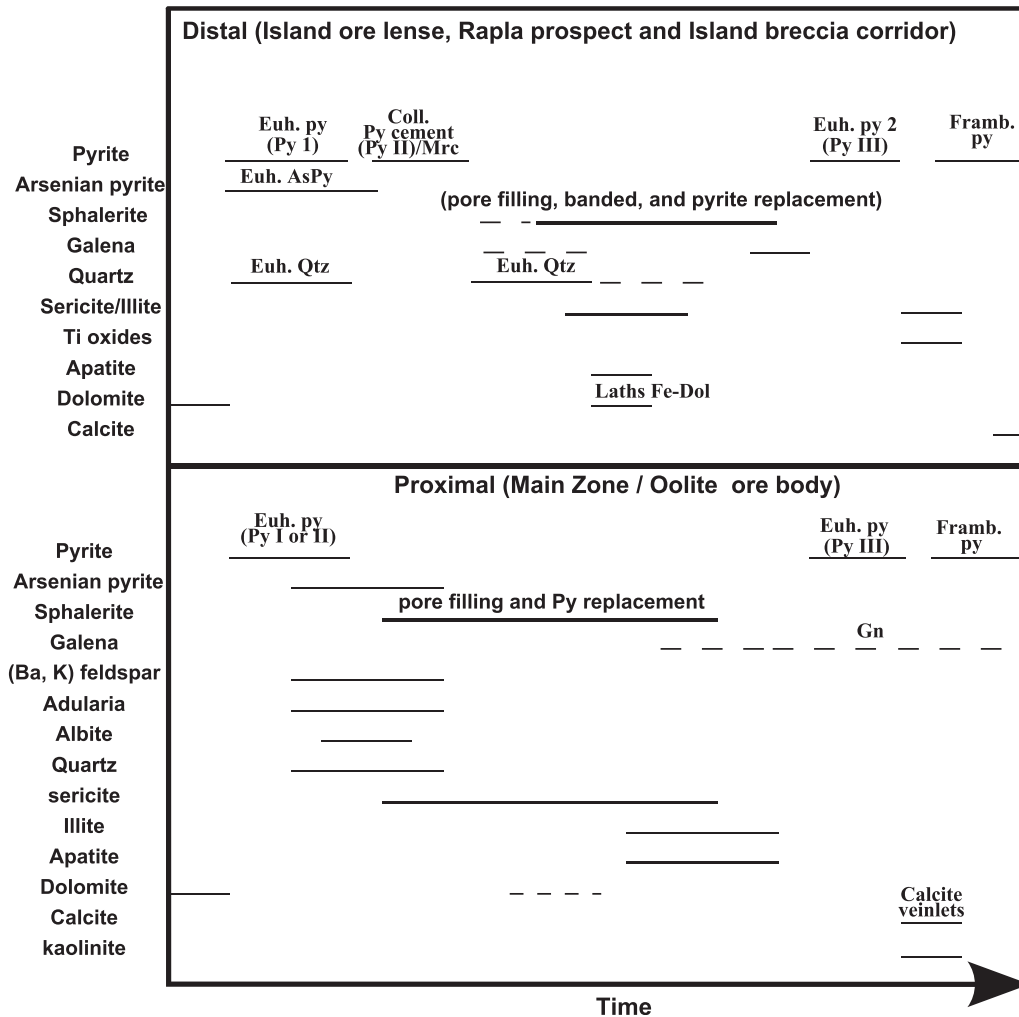


Fig. 9. Paragenetic summary of mineral relationships (Proximal-Distal) along the Rathdowney Trend as interpreted for samples from the Lisheen deposit and Rapla occurrence.

feldspars would imply a lower pH for the hydrothermal fluid, which could explain the illitization features observed for feldspars at the Lisheen Main Zone.

In addition, variations in the potassic gangue mineral assemblages observed from the distal ore pod of the Island to the south-east part of the Main Zone orebody, evolving from an illitic signature to a more illite/phengite mix, where the latter appears to be predominant, as well as the occurrence of hydrothermal feldspar may indicate either an evolution in the fluid properties as the distance to the feeder zone (array of main normal faults) increases or hydrothermal pulses of different physiochemical fluid conditions (eH, and pH). Similarly the occurrence of feldspars in the relative vicinity of the Killoran fault, the main normal fault bounding the Lisheen Main Zone ore body, would indicate either a higher temperature or a more potassic fluid, and the presence of a significant conduit for hydrothermal fluids carrying Si, Al, and K as well as base metals. This would also be in good agreement with the models of (Hitzman and Beaty, 1996; Russell, 1978; Wilkinson et al., 2005a) involving brine interaction within the sub-basin basement rock to leach and transport not only ore metals, but K and Ba as well. The interpretation of the normal fault zones located south of the Lisheen Main Zone is that of a feeder conduit for ore fluids responsible for the base-metal mineralization with a metal zonation of Ni, Cu, Pb proximal to the feeder and Zn and Fe occurring distally (Fusciardi et al., 2003; Torremans et al., 2017). Metal zonation with Fe indicating higher temperature and metal zonation in

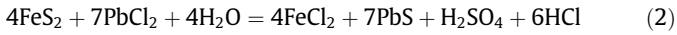
MVT deposits (Marie et al., 2001), highlights the complex fluid flows and the need of integration between geochemistry, mineralogy and dynamic structural (4D) models to better understand geochemical zonation in carbonate hosted deposits.

### 5.2. Ore texture, paragenesis, and massive sulfide precipitation processes

Ore textures can be used to help constrain possible mechanisms of precipitation e.g. pH variations inducing dissolution of the gangue minerals, presence of organic compounds, or other processes resulting from dilution or a decrease in temperature (Roedder, 1968). On the basis of petrographic, geochemical and isotopic evidence, numerous authors have advocated for a binary (two fluid) model involving a metalliferous hydrothermal fluid mixing with a fluid containing reduced (bacteriogenic) sulfide in dolomitized carbonate reef limestones of the Irish Midlands (Wilkinson et al., 2005a).

Textural evidence of FeS<sub>2</sub> replacement by sphalerite and neoformed sphalerite filling the porosity together with the occurrence of barian-feldspars suggests the presence of an acidic fluid with low SO<sub>4</sub><sup>2-</sup> contents, limiting barite precipitation. This is in agreement with isotopic and fluid inclusion data, which favors a mixing mechanism to precipitate base metal sulfides from H<sub>2</sub>S in solution or via the replacement of FeS<sub>2</sub> (Wilkinson et al., 2005a, 2011; Hitzman and Beaty, 1996). Given the aforementioned constraints,

the following reactions may be considered to describe the metal precipitation from hydrothermal fluids along the Rathdowney Trend, as considered in (Anderson, 1975; Anderson and Garven, 1987; Lovering, 1961), and compared in a mineral and sulfate/sulfur, equilibrium Eh/pH diagram in Fig. 10. Eqs. (1) and (2) illustrating the precipitation of massive sulfide (MS) from a mixing and replacement mechanism, respectively:



In the absence of metal ions, the ascending brine will inevitably become oxidized (Eq. (3)), while a decrease in pH will favor the formation of illite or phengite over feldspars in Eq. (4):



Variability in feldspar and phyllosilicate abundance could be driven by several mechanisms. The phyllosilicates may be controlled by the acidity of the ore fluid or  $H^+$  generated during sulfide precipitation, which in both cases would lead to the precipitation of potassic phyllosilicate minerals in the black matrix breccias as well as contribute to the dissolution of the host rock. This could also be an effect of the fluid rock ratio dependent upon the volume of sulfide replaced or precipitated (see Eqs. (1) and (2)). Ultimately, the neutralization of the fluid would be coincident with both the precipitation of feldspar in near equilibrium with carbonate phases in the black matrix breccias as evidenced from petrographic relationships.

### 5.3. Alteration, massive sulfide precipitation and breccias development

Petrographic study of breccias along the Rathdowney Trend have revealed evidence of a strong chemical corrosion (brecciation) factor, to produce fragments with a medium to high fractal dimen-

sion ( $D_r > 1.1$ ). The limited spread in the fractal dimension values might originate in the progressive generation of clasts via dissolution likely originating from discontinuities such as microfractures or stylolitic joints (alone or as mechanical protobreccias), and indicates the predominance of chemical corrosion to produce fragments with very complex contours. These heterogeneities resulted in the constant addition of newly detached fragments to the breccias during collapse processes. Fractal analysis has also provided a better visualization of the distribution of hydrothermal silicate (quartz) precipitating throughout the matrix. The use of large-scale chemical maps then becomes essential to link the texture of fragments to the mineralogy of the matrix. Textural analysis confirms previous observations indicating the hydrothermal nature of the black matrix breccias resulting from dissolution of the original carbonate and partial replacement by hydrothermal dolomite (Hitzman et al., 1992, 2002; Wilkinson et al., 2011). In addition, Wilkinson et al. (2011) have shown that the clasts were similarly affected by fluid rock alteration, but to a lesser degree than the matrix, a feature confirmed herein through chemical mapping of homogeneous clasts exhibiting highly corroded edges. With the establishment of a paragenetic association between the phyllosilicates (illite) and the massive sulfide ore, a genetic link between hydrothermal mineralization processes and the development of black matrix breccias may be discussed from a mineralogical point of view. The chemical disequilibrium generating the black matrix breccias could not only be due to the influx of the hot acidic hydrothermal fluids into dolomitized Waulsortian carbonates, but the breccias could be enhanced by local variations in pH during the precipitation of sulfide minerals. Indeed, sphalerite neof ormation in the porosity of the dolomitized limestone or the replacement of iron sulfide mineral forms already present in the host rock can lead to the production of  $H^+$  and a decrease in pH. For a partially fracture-controlled reservoir, the fluid will not necessarily react pervasively with the host rock and may preferentially follow a fracture network composed of breccias and fracturation corridors. This may lead to locally high disequilibrium, with the buffering role of the host carbonate sequence being

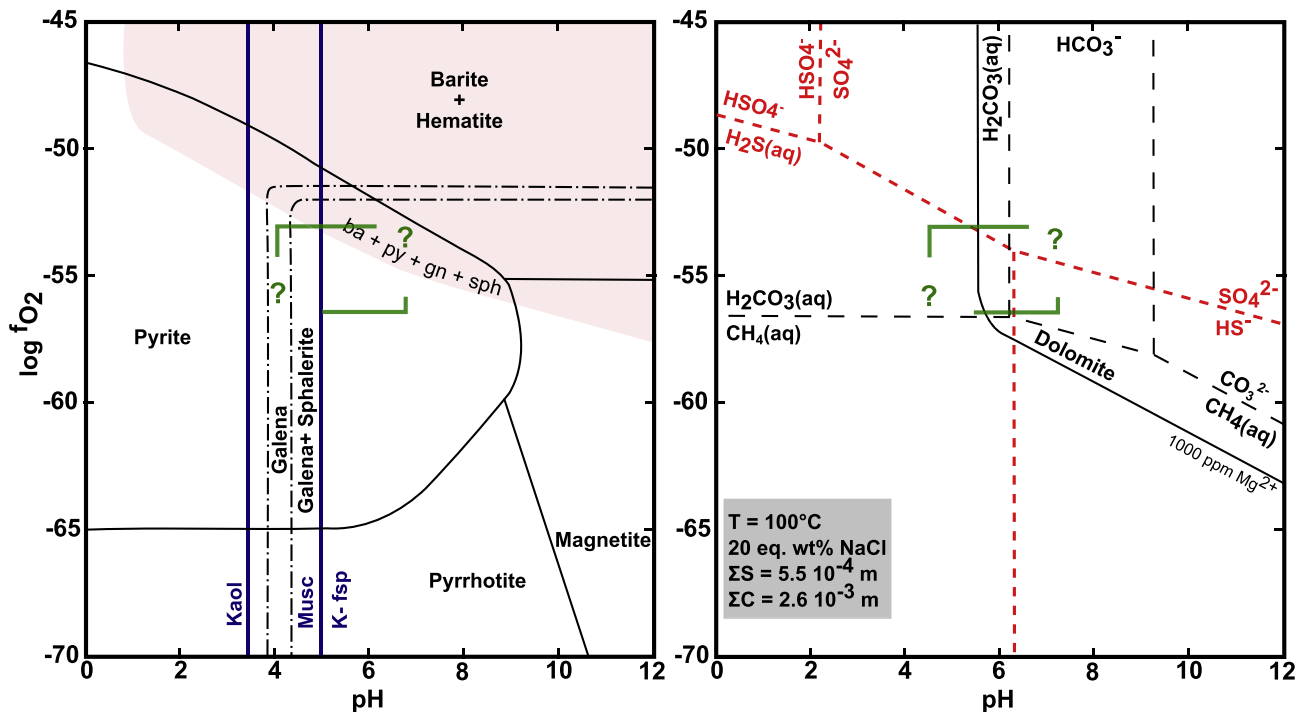


Fig. 10. Eh vs pH diagram modified from (Cooke et al. 1998) and (Hanor, 2000), representing the field of stabilities of sulfides, carbonate and aqueous species, as well as silicates at 100 °C. The green box represents the possible range of composition deduced from the petrography and the mineral assemblages.

limited to the fluid-rock ratio. This may explain the close spatial association between massive sulfide lenses and the enveloping black matrix breccias. Furthermore, the flow of residual fluids away from the site of massive sulfide deposition might be able to produce large corridors of black matrix breccias without a direct association to Zn-Pb mineralization. Such features could then be used to reconstruct the paleofluid circulation at the time of ore deposition from the feeder zones, to more distal areas where metals have been progressively removed from the fluid while  $K^+$  and  $H^+$  could continue to facilitate hydrothermal breccia development. The black matrix breccias can be seen as dynamic markers of the hydrothermal system, as a consequence of the ore formation processes and also contributing to the formation of volume for subsequent mineralization events through host rock dissolution.

## 6. Concluding remarks

The present work has shown that, despite a different tectonic context to their North American MVT counterparts (see Wilkinson, 2014 and references therein), the Irish type carbonate-hosted base metal metallogenic province shares similar alteration features, in particular, the presence of potassic silicates that are cogenetic with massive sulfide mineralization. These mineral assemblages can help to define zonation and the lateral expression of fluid-rock reaction pathways, to complement bulk lithogeochemical approaches proposed by Wilkinson et al. (2011). These results can be integrated with structural models being developed for the Irish Midlands to understand the hydrothermal architecture in a more dynamic fashion.

The stability of barian feldspar over barite would indicate generally higher temperatures and reducing conditions, compatible with conditions envisaged for hydrothermal feeder conduits. It also supports genetic models requiring the hydrothermal leaching (brine) and remobilization of metals from the basement and subsequent mixing with a disparate reservoir of reduced (bacteriogenic) sulfur in an open system (Hitzman and Beaty, 1996; Russell, 1978; Wilkinson et al., 2005a). This together with the occurrence of potassic phyllosilicate minerals (illite and phengite) would suggest that regional lithogeochemical research should investigate the relationship between Si, Al, Ba and K, and not necessarily attribute barium anomalies to the simple occurrence of barite. This could help vector towards the feeder systems of the ore bodies, to reveal zones where deep, hot, metalliferous brines ascending along large normal faults are predominant over seawater derived fluids containing reduced sulfur. Interestingly, the relative abundance of barium feldspar over barite could be used as a marker for proximity to feeder zones of the deposits, while illite and phengite may indicate either distal occurrences and/or mildly acidic conditions. Consequently, this may account for some occurrences of black matrix breccias with or without massive Zn-Pb mineralization. They would rather show the pathway of a depleted fluid progressing past the sulfide precipitation front. The spatial relationship between the black matrix breccias in apparently barren regions of the Rathdowney Trend and the relative position of known ore bodies could then be investigated to understand the paleoplumbing system at the time of deposit formation.

The constrained gangue mineral assemblage, coupled with thermodynamic data, as well as the projected geometry of breccias relative to ore bodies along the Rathdowney Trend, suggests that the black matrix breccias may not solely originate from the chemical corrosion induced by the primary ore fluid alone. Their formation could be assisted by an evolved (depleted) hydrothermal fluid resulting from sulfide precipitation processes inducing phyllosilicate neof ormation and local acidification that could also produce chemical brecciation. In addition to the fracturation processes

creating the necessary focus conduits for the fluids, such a mechanism could also create space for the mineralization and maintain the hydraulic conductivity via dissolution and collapse processes.

Given the importance of the potassic silicate mineralogy as a marker of hydrothermal conditions in carbonate-hosted Zn-Pb deposits, these subtle occurrences should be more scrutinized. They could provide a possible guide for the mineral exploration industry and contribute to a re-evaluation of the bulk lithogeochemical approach for exploration within the Irish Midlands. Then, a normative approach to the mineralogy of K and Ba phases could potentially provide vectors to mineralization and the identification of feeder zones for new and existing deposits.

## Acknowledgments

We would like to express our gratitude toward John Güven and iCRAG colleagues for the constructive discussions throughout of the project and to Oakley Turner for providing comments and map figures. We would also like to thank Vedanta Exploration for access to samples, and in kind logistical support. We are grateful to Professor Daniel Beaufort and Professor Alain Meunier for their constructive comments and insightful discussion on the clay mineralogy. The first author would like to thank Dr Christophe Bonnetti for fruitful discussions. The constructive comments of Professor Michel Jébrak, an anonymous referee and Ore Geology Reviews editor Professor Franco Pirajno referee are gratefully acknowledged. This publication has emanated from research supported in part by a research grant from Science Foundation Ireland (SFI) under Grant Number 13/RC/2092 and is co-funded under the European Regional Development Fund and by iCRAG industry partners.

## References

- Anderson, G.M., 1975. Precipitation of mississippi valley-type ores. *Econ. Geol.* 70, 937–942.
- Anderson, G.M., Garven, G., 1987. Sulfate-sulfide-carbonate associations in mississippi valley-type lead-zinc deposits. *Econ. Geol.* 82, 482–488.
- Banks, D.A., Boyce, A.J., Samson, I.M., 2002. Constraints on the origins of fluids forming Irish Zn-Pb-Ba deposits: evidence from the composition of fluid inclusions. *Econ. Geol.* 97, 471–480.
- Barnes, H.L., 1979. Solubilities of ore minerals. In: Barnes, H.L. (Ed.), *Geochemistry of Hydrothermal Ore Deposits*. Wiley-Interscience, New York, p. 787.
- Bérubé, D., Jébrak, M., 1999. High precision boundary fractal analysis for shape characterization. *Comput. Geosci.* 25, 1059–1071.
- Blenkinsop, T.G., 1991. Cataclasis and processes of particle size reduction. *Pure Appl. Geophys.* 136, 59–86.
- Chabu, M., Boulegue, J., 1992. Barian feldspar and muscovite from the Kipushi Zn-Pb-Cu deposit, Shaba, Zaire. *Can. Mineral.* 30, 1143–1152.
- Coats, J.S., Fortey, N.J., Gallagher, M.J., May, F., McCourt, W.J., 1980. Strata-bound barium-zinc mineralization in Dalradian schist near Aberfeldy, Scotland. *Trans. Inst. Min. Metall. Sect. B Appl. Earth Sci.* 89, 110–122.
- Cooke, D.R., Bull, S.W., Donovan, S., Rogers, J.R., 1998. K-metasomatism and base metal depletion in volcanic rocks from the McArthur Basin, Northern Territory; implications for base metal mineralization. *Econ. Geol.* 93, 1237–1263.
- Cruise, M.D., 2000. Iron oxides and associated base metal mineralization in the Central Midlands Basin, Ireland (Unpublished Ph.D. thesis). Trinity College, Dublin, p. 651.
- Deer, W.A., Howie, R.A., Zussman, J., 2001. *Rock-Forming Minerals: Feldspars*, vol. 4A. Geological Society.
- Dong, G., Morrison, G.W., 1995. Adularia in epithermal veins, Queensland: morphology, structural state and origin. *Miner. Deposita* 30, 11–19.
- Doyle, E., Bowden, A., 1995. Fieldguide to the Galmoy zinc-lead deposits. In: Anderson, K, Ashton, J, Earls, G, Hitzman, MW, Tear, S (Eds.), *Carbonate-Hosted Zn-Pb Deposits*. Society of Economic Geologists, pp. 139–145.
- Doyle, E., Bowden, A.A., Jones, G.V., Stanley, G.A., 1992. The geology of the Galmoy deposit. In: Bowden, A., Earls, G., O'Connor, P., Pyne, J. (Eds.), *The Irish Mineral Industry 1980–1990*. Irish Association for Economic Geology, Dublin.
- Eyre, S.L., 1998. *Geochemistry of Dolomitization and Pb-Zn Mineralization in the Rathdowney Trend*. University of London, Ireland. London, p. 414.
- Fortey, N.J., Beddoe-Stephens, B., 1982. Barium silicates in stratabound Ba-Zn mineralization in the Scottish Dalradian. *Mineral. Mag.* 46, 63–72.
- Fusciardi, L.P., Güven, J., Stewart, D.R.A., Carboni, V., Walsh, J.J., 2003. The geology and genesis of the Lisheen Zn-Pb deposit, Co., Tipperary, Ireland. In: Kelly, J.C., Andrew, J.H., Ashton, J., Boland, M.B., Fusciardi, L., Stanley, G.A. (Eds.), *Europe's Major Base Metal Deposits*. Irish association for economic geology.

- Gay, P., Roy, N.N., 1968. Mineralogy of potassium-barium feldspars series.3. Subsolidus relationships. *Mineral. Mag. J. Mineral. Soc.* 36, 914.
- Giordano, T.H., 1985. A preliminary evaluation of organic ligands and metal-organic complexing in mississippi valley-type ore solutions. *Econ. Geol.* 80, 96–106.
- Giordano, T.H., Barnes, H.L., 1981. Lead transport in mississippi valley-type ore solutions. *Econ. Geol.* 76, 2200–2211.
- Hanor, J.S., 2000. Barite-celestine geochemistry and environments of formation. *Rev. Mineral. Geochem.* 40, 193–275.
- Heald, P., Foley, N.K., Hayba, D.O., 1987. Comparative anatomy of volcanic-hosted epithermal deposits; acid-sulfate and adularia-sericite types. *Econ. Geol.* 82, 1–26.
- Hearn, P.P., Sutter, J.F., 1985. Authigenic potassium feldspar in Cambrian carbonates: evidence of alleghanian brine migration. *Science* 228, 1529–1531.
- Hearn, P.P., Sutter, J.F., Belkin, H.E., 1987. Evidence for Late-Paleozoic brine migration in Cambrian carbonate rocks of the central and southern Appalachians: implications for Mississippi Valley-type sulfide mineralization. *Geochim. Cosmochim. Acta* 51, 1323–1334.
- Hemley, J.J., 1959. Some mineralogical equilibria in the system  $K_2O-Al_2O_3-SiO_2-H_2O$ . *Am. J. Sci.* 257, 241–270.
- Hemley, J.J., Jones, W.R., 1964. Chemical aspects of hydrothermal alteration with emphasis on hydrogen metasomatism. *Econ. Geol.* 59, 538–569.
- Héroux, Y., Chagnon, A., Dewing, K., Rose, H.R., 2000. The carbonate-hosted base-metal sulphide Polaris deposit in the Canadian Arctic: organic matter alteration and clay diagenesis. In: Glikson, M., Mastalerz, M. (Eds.), *Organic Matter and Mineralisation: Thermal Alteration, Hydrocarbon Generation and Role in Metallogenesis*. Springer, Dordrecht, Netherlands, pp. 260–295.
- Heyl, A.V., Hosterman, J.W., Brock, M.R., 1964. Clay mineral alteration in the Upper Mississippi Valley zinc-lead district. *Clays and clay minerals*. 12th Natl Conf. Macmillan, Atlanta, pp. 445–453.
- Hitzman, M.W., Beaty, D.W., 1996. The Irish Pb-Zn-(Ba) orefield. In: Sangster, D.F. (Ed.), *Carbonate-Hosted Lead-Zinc Deposits*. Society of Economic Geologists, pp. 112–143.
- Hitzman, M.W., Large, D., 1986. A review and classification of the Irish carbonate-hosted base metal deposits. *Geology and genesis of mineral deposits in Ireland: Dublin, Irish. Assoc. Econ. Geol.*, 217–238
- Hitzman, M.W., O'Connor, P., Shearley, E., Schaffalitzky, C., Beaty, D.W., Allan, J.R., et al., 1992. Discovery and geology of the Lisheen Zn-Pb-Ag prospect, Rathdowney Trend, Ireland. In: Bowden, A., Earls, G., O'Connor, P., Pyne, J. (Eds.), *The Irish Minerals Industry 1980–1990*. Irish Association for Economic Geology, Dublin, pp. 227–246.
- Hitzman, M.W., Redmond, P.B., Beaty, D.W., 2002. The carbonate-hosted Lisheen Zn-Pb-Ag deposit, County Tipperary, Ireland. *Econ. Geol.* 97, 1627–1655.
- Jébrak, M., 1997. Hydrothermal breccias in vein-type ore deposits: a review of mechanisms, morphology and size distribution. *Ore Geol. Rev.* 12, 111–134.
- Johnson, A.W., Shelton, K.L., Gregg, J.M., Somerville, I.D., Wright, W.R., Nagy, Z.R., 2009. Regional studies of dolomites and their included fluids: recognizing multiple chemically distinct fluids during the complex diagenetic history of Lower Carboniferous (Mississippian) rocks of the Irish Zn-Pb ore field. *Mineral. Petrol.* 96, 1–18.
- Johnston, J.D., 1999. Regional fluid flow and the genesis of Irish Carboniferous base metal deposits. *Miner. Deposita* 34, 571–598.
- Johnston, J.D., Coller, D., Millar, G., Critchley, M.F., 1996. Basement structural controls on Carboniferous-hosted base metal mineral deposits in Ireland. *Geol. Soc. London Spec. Publ.* 107, 1–21.
- Kontak, D.J., Farrar, E., McBride, S.L., 1994. 40 Ar/ 39 Ar dating of fluid migration in a mississippi valley-type deposit; the Gays River Zn-Pb deposit, Nova Scotia, Canada. *Econ. Geol.* 89, 1501–1517.
- Kribeek, B., Hladikova, J., Zak, K., Bendl, J., Pudilova, M., Uhlík, Z., 1996. Barite-hyalophane sulfidic ores at Rozna, Bohemian Massif, Czech Republic; metamorphosed black shale-hosted submarine exhalative mineralization. *Econ. Geol.* 91, 14–35.
- Kucha, H., 1988. Zn-Pb sulfides as rim cements, filling cements and replacement of carbonate sediments, Moyvoughly, Ireland. *Trans. Inst. Min. Metall.* 97, 64–76.
- Kyne, R., Torremans, K., Doyle, E., Güven, J., Walsh, J., 2017. The Role of Fault Segmentation and Relay Ramp Geometries on the Formation of Irish-Type Deposits. Joint assembly of TSG-VMSC-BGA, Liverpool, England.
- Leach, D.L., Rowan, E.L., 1986. Genetic link between Ouachita foldbelt tectonism and the Mississippi Valley-type lead-zinc deposits of the Ozarks. *Geology* 14, 931–935.
- Leach, D.L., Sangster, D.F., 1993. Mississippi Valley-type lead zinc deposits. In: Kirkham, R.V., Duke, J.M., Sinclair, A.J., Thorpe, R.I. (Eds.), *Mineral Deposits Modelling*. Geological Association of Canada, pp. 289–314.
- Leach, D.L., Taylor R.D., Fey D.L., Diehl S.F., Saltus R.W. A deposit model for Mississippi Valley-Type lead-zinc ores: Chapter A in Mineral deposit models for resource assessment. Scientific Investigations Report. Reston, VA2010.
- Lovering, T.S., 1961. Sulfide ores formed from sulfide-deficient solutions. *Econ. Geol.* 56, 68–99.
- Mallon, A.J., 1997. Petrological and mineral characteristics of the Old Red Sandstone facies rocks beneath base metal deposits as a guide to the setting of mineralization in the Irish Midlands (Unpublished PhD thesis). University College Cork, Cork, p. 636.
- Marcoux, E., Pélissou, P., Baubron, J.-C., Lhégu, J., Touray, J.-C., 1990. Âges des formations filoniennes à fluorine-barytine-quartz du district de Paulhaguet (Haute-Loire, Massif Central Français). *Comptes rendus de l'Académie des sciences Série 2. Mécanique, Physique, Chimie, Sciences de l'univers, Sciences de la Terre.* 311, 829–835.
- Marie, J.S., Kesler, S.E., Allen, C.R., 2001. Origin of iron-rich Mississippi Valley-type deposits. *Geology* 29, 59–62.
- Marignac, C., 1988. A case of ore deposition associated with paleogeothermal activity: the polymetallic ore veins of Ain Barbar (NE Constantinois, Algeria). *Mineral. Petrol.* 39, 107–127.
- McSwiggen, P.L., Morey, G.B., Cleland, J.M., 1994. Occurrence and genetic implications of hyalophane in manganese-rich iron-formation, Cuyuna Iron Range, Minnesota, USA. *Mineral. Mag.* 58, 387–399.
- Meunier, A., Velde, B., 1982. Phengitization, sericitization and potassium-beidellite in a hydrothermally altered granite. *Clay Miner.* 17, 285–299.
- Meunier, A., Velde, B., 1989. Solid solutions in I/S mixed-layer minerals and illite. *Am. Mineral.* 74, 1106–1112.
- Meunier, A., Velde, B., 2004. *Illite*. Springer-Verlag, Berlin Heidelberg.
- Moro, M.C., Cembranos, M.L., Fernandez, A., 2001. Celsian, (Ba, K)-feldsAnd cymrite from sedex barite deposits of Zamora, Spain. *Can. Mineral.* 39, 1039–1051.
- Philcox, M.E., 1984. Lower carboniferous lithostratigraphy of the Irish midlands. *Irish Association for Economic Geology, Dublin*, p. 89.
- Pouit, G., Bois, J.-P., 1986. Arrens Zn (Pb), Ba devonian deposit, Pyrénées, France: an exhalative-sedimentary-type deposit similar to Meggen. *Miner. Deposita* 21, 181–189.
- Redmond, P., 1997. Structurally Controlled Mineralization and Hydrothermal Dolomitization and the Lisheen Zn-Pb-Ag Deposit, Co., Tipperary (Ireland Unpublished M.Sc. thesis). Dublin University, Trinity College, p. 126.
- Reed, C.P., Wallace, M.W., 2004. Zn-Pb mineralisation in the Silvermines district, Ireland: a product of burial diagenesis. *Miner. Deposita* 39, 87–102.
- Rieder, M., Cavazzini, G., D'yakov, Y.S., Frank-Kamenetskii, V.A., Gottardi, G., Guggenheim, S., et al., 1998. Nomenclature of the micas. *Can. Mineral.* 36, 905–912.
- Roedder, E., 1968. The non-colloidal origin of 'colloform' textures in sphalerite ores. *Econ. Geol.* 63, 451–471.
- Rosenberg, P.E., 2002. The nature, formation, and stability of end-member illite: a hypothesis. *Am. Mineral.* 87, 103–107.
- Rothbard, D.R., 1983. Diagenetic history of the Lamotte Sandstone, southeast Missouri. In: Kisvarsanyi, G. (Ed.), *International conference on Mississippi Valley-type lead-zinc deposits*. University of Missouri, Rolla, pp. 385–395.
- Russell, M. Downward-EXcavating hydrothermal cells and irish-type ore-deposits-importance of an underlying thick caledonian prism. *Inst mining metallurgy 44 portland place, London, England W1n 4BR; 1978. pp. B168–B71.*
- Sangster, D.F., 1996. Mississippi Valley-type lead zinc deposit. In: Eckstrand, O.R., Sinclair, A.J., Thorpe, R.I. (Eds.), *Geology of Canadian mineral deposits types*. Geological Survey of Canada, Ottawa, pp. 253–261.
- Sartorius von Walterhausen, W., 1855. Ein Beitrag zur näheren Kenntniss des Dolomits in der Walliser Alpen. *Ann Phys Chem (Poggendorf)*, 94–115.
- Schneider, C.A., Rasband, W.S., Eliceiri, K.W., 2012. NIH Image to ImageJ: 25 years of image analysis. *Nat Meth.* 9, 671–675.
- Seedorf, E., Dilles, J.H., Proffett Jr., J.M., Einaudi, M.T., Zurcher, L., Stavast, W.J.A., et al., 2005. Porphyry Deposits: characteristics and origin of hypogene features. In: Hedenquist, J.W., Thompson, J.F.H., Goldfarb, R.J., Richards, J.P. (Eds.), *Economic Geology 100th Anniversary Volume*. Society of Economic Geology, pp. 251–298.
- Segnit, E.R., 1942. Barium-feldspars from Broken Hill, Vol. 27. *Mineralogical Magazine, New South Wales*, pp. 166–174.
- Shearley, E., Hitzman, M.W., Walton, G., Redmond, P., Davis, R., King, M., et al., 1992. Structural Controls of Mineralization, Lisheen Zn-Pb-Ag Deposit, Co., Tipperary, Ireland. *Geological Society of America*, p. 354.
- Shelton, K.L., Reader, J.M., Ross, L.M., Viele, G.W., Seidemann, D.E., 1986. Ba-rich adularia from the Ouachita Mountains, Arkansas; Implications for a postcollisional hydrothermal system. *Am Mineral.* 71, 916–923.
- Smith, J.V., Brown, W.L., 1988. *FeldsMinerals. 1 Crystal structures, physical, chemical, and microtextural properties.* Springer Verlag, Heidelberg New York London Paris Tokyo, p. 828.
- Stormo, S., Sverjensky, D.A., 1983. Silicate hydrothermal alteration in a Mississippi Valley-type deposit, Viburnum, southeast Missouri. *Geol. Soc. Am.*, 699
- Sverjensky, D.A., 1984. Europium redox equilibria in aqueous solution. *Earth Planet. Sci. Lett.* 67, 70–78.
- Sverjensky, D.A., 1986. Genesis of Mississippi Valley-type lead-zinc desposits. *Annu. Rev. Earth Planet. Sci.* 14, 177–199.
- Torremans, K., Kyne, R., Doyle, R., Güven, J., Walsh, J., 2017. Fluid Flow, Feeders and Fault Zone Structure – Controls on Metal Distributions in Irish-Type Deposits. Joint Assembly of TSG-VMSC-BGA, Liverpool, England.
- Turner, O., Riegler, T., Güven, J., McClenaghan, S.H., 2016. Chemostratigraphy and geochemical vectoring at the Rapla prospect, Rathdowney trend, Ireland, 35th International Geological Conference. Cape Town, South Africa.
- Wilkinson, J.J., 2003. On diagenesis, dolomitisation and mineralisation in the Irish Zn-Pb orefield. *Miner Deposita* 38, 968–983.
- Wilkinson, J.J., 2010. A review of fluid inclusion constraints on mineralization in the Irish ore field and implications for the genesis of sediment-hosted Zn-Pb deposits. *Econ Geol.* 105, 417–442.
- Wilkinson, J.J., 2014. 13.9 – Sediment-Hosted zinc-lead mineralization: processes and perspectives A2 - Holland, Heinrich D. In: Turekian, K.K. (Ed.), *Treatise on Geochemistry*. second ed. Elsevier, Oxford, pp. 219–249.
- Wilkinson, J.J., Earls, G., 2000. A high-temperature hydrothermal origin for black dolomite matrix breccias in the Irish Zn-Pb orefield. *Mineral. Mag.* 64, 1017–1036.

- Wilkinson, J.J., Everett, C.E., Boyce, A.J., Gleeson, S.A., Rye, D.M., 2005a. Intracratonic crustal seawater circulation and the genesis of subseafloor zinc-lead mineralization in the Irish orefield. *Geology* 33, 805–808.
- Wilkinson, J.J., Eyre, S.L., Boyce, A.J., 2005b. Ore-forming processes in Irish-type carbonate-hosted Zn-Pb deposits: evidence from mineralogy, chemistry, and isotopic composition of sulfides at the Lisheen Mine. *Econ Geol.* 100, 63–86.
- Wilkinson, J.J., Crowther, H.L., Coles, B.J., 2011. Chemical mass transfer during hydrothermal alteration of carbonates: controls of seafloor subsidence, sedimentation and Zn-Pb mineralization in the Irish Carboniferous. *Chem. Geol.* 289, 55–75.
- Wilkinson, J.J., Hitzman, M.W., 2015. The Irish Pb-Zn orefield: the view from 2014. In: Archibald, S.M., Piercey, S.J. (Eds.), *Current Perspective on Zinc Deposits*. Irish Association for Economic Geology, pp. 59–72.